

8-2021

DISSECTING THE MECHANISMS OF VENETOCLAX RESISTANCE IN MYELODYSPLASTIC SYNDROMES

Shuaitong Chen

Follow this and additional works at: https://digitalcommons.library.tmc.edu/utgsbs_dissertations



Part of the [Medicine and Health Sciences Commons](#)

Recommended Citation

Chen, Shuaitong, "DISSECTING THE MECHANISMS OF VENETOCLAX RESISTANCE IN MYELODYSPLASTIC SYNDROMES" (2021). *The University of Texas MD Anderson Cancer Center UTHealth Graduate School of Biomedical Sciences Dissertations and Theses (Open Access)*. 1124.
https://digitalcommons.library.tmc.edu/utgsbs_dissertations/1124

This Thesis (MS) is brought to you for free and open access by the The University of Texas MD Anderson Cancer Center UTHealth Graduate School of Biomedical Sciences at DigitalCommons@TMC. It has been accepted for inclusion in The University of Texas MD Anderson Cancer Center UTHealth Graduate School of Biomedical Sciences Dissertations and Theses (Open Access) by an authorized administrator of DigitalCommons@TMC. For more information, please contact digitalcommons@library.tmc.edu.

DISSECTING THE MECHANISMS OF VENETOCLAX RESISTANCE IN MYELOYDYSPLASTIC
SYNDROMES

Shuaitong Chen, B.A.

APPROVED:

Simona Colla, Ph.D.
Advisory Professor

Marina Konopleva, M.D., Ph.D.

Stephanie Watowich, Ph.D.

Koichi Takahashi, M.D., Ph.D.

George Calin, Ph.D.

Guocan Wang, Ph.D.

APPROVED:

Dean, The University of Texas
MD Anderson Cancer Center UTHealth Graduate School of Biomedical Sciences

DISSECTING THE MECHANISMS OF VENETOCLAX RESISTANCE IN MYELODYSPLASTIC
SYNDROMES

A
THESIS

Presented to the Faculty of
The University of Texas
MD Anderson Cancer Center UTHealth
Graduate School of Biomedical Sciences
In Partial Fulfillment
of the Requirements
for the Degree of
MASTER OF SCIENCE

By
Shuaitong Chen, B.A.
Houston, Texas
August 2021

This work is dedicated to my dearest family
for their unconditional love and support

ACKNOWLEDGEMENTS

Many people have given me an enormous amount of encouragement and support during the path to degree completion. I am indebted to them, and they deserve more than being highlighted here. First and foremost, I would like to thank my mentor, a brilliant scientist, Dr. Simona Colla, for sponsoring my graduate study and the extensive training and enlightening guidance she provided to me throughout these two years. I am always inspired by your intelligence and passion in science, your endeavors, efficiency, persistence, and exceptional powers of concentration as the key to becoming a successful woman in science, and your remarkable capacity for work and operation of the lab. I have learned a lot from you. How lucky am I to have you as my mentor, be in the Colla lab, and participate in the Moonshot project you are leading? I could not have asked for a better mentor and a better lab. Thank you so much for always being so supportive and enthusiastic, which has helped me come through stressful and sorrowful moments in my life. Thank you so much for trusting me and pushing me to become more confident and professional! I could not make any of the improvements that I have achieved without your support.

Then, thanks to my role model Dr. Irene Gañan-Gomez, an outstanding scientist who has provided me a considerable amount of hands-on laboratory experience. I am sincerely amazed by your high levels of independence, orderliness, carefulness, and determinacy. How many times have I seen you make mistakes? ZERO. These have pushed me to work hard to keep up with your level. Thank you for always being so energetic and thoughtful! I am so lucky to work with you in pursuit of a career in clinical research.

To Nat, Vera, Pam, Andrea, Naran, Ashley, and Chris in the Colla lab – you all are one of those most adorable people on the planet. Besides the science that you all have helped me with, I have really enjoyed talking to you sharing all kinds of stories in life. Thank you, Nat, for being my cat and tennis buddy. Animals and sports are always healing. Thank you, Vera, for always sharing funny stories and organizing activities outside. The waves of laughter we have

had are unforgettable. Thank you, Pam, for keeping the lab organized and sharing anatomy during dissection in a fun way. Thank you, Andrea, for your touches of sarcasm which kept the conversation amusing. Thank you, Naran, for taking care of our precious mice. Thank you, Ashley and Chris, for teaching me the basics in the laboratory. Hanging out with you all has been the most enjoyable and healing thing in the world. Again, how lucky am I to be in the Colla lab family? And thank you, Kelly! I really appreciate your time and assistance in improving the correctness and clarity of all my written works. I could not ask for better advice. You are truly wonderful.

My graduate study is also with excellent guidance of my distinguished advisory committee members – Dr. Marina Konopleva, Dr. Stephanie Watowich, Dr. Koichi Takahashi, Dr. George Calin, and Dr. Guocan Wang. Thank you all so much for always being so thoughtful and helpful. The significance of this project has been considerably improved owing to your comments and suggestions. I really appreciate your time and attention during each committee meeting.

For sure, it would be impossible for me to pursue a career in Cancer Biology here without my family's unconditional support. Since the moment they allowed me to leave behind the admission to a university in my home country and come to the US for a career in biological study, it had been a substantial financial burden for them. Thank you so much for approving my bold decision and your devotion to ensure that I am working on the subjects that I am truly interested in. Words just cannot express my gratitude and love to all of you.

Lastly, thanks to all my friends that I have met in Houston. I have had lots of fun exploring the city with you all. Before I came here, I never thought that my life would be so rich and colorful. You are all scientists with a bright future and my best buddies for exploring food, coffee shops, game nights, sports, museums, etc. I am incredibly grateful to all of you.

DISSECTING THE MECHANISMS OF VENETOCLAX RESISTANCE IN MYELOYDYSPLASTIC SYNDROMES

Shuaitong Chen, B.A.

Advisor: Simona Colla, Ph.D.

Myelodysplastic syndromes (MDS) are a class of heterogeneous clonal hematopoietic disorders. The current standard of care for MDS is the hypomethylating agent (HMA)-based therapy. However, only 50 percent of the patients respond, with transient effects and no approved second-line treatment options after their diseases progress to acute myeloid leukemia (AML). The mechanisms that govern HMA failure are unknown. Recently, we unveiled that MDS are maintained and propagated by two different immunophenotypically distinct hierarchical cellular organizations of MDS hematopoietic stem and progenitor cells (HSPCs) through the upregulation of specific survival pathways. This finding allowed us to potentially stratify MDS patients into two subgroups for more effective guided therapy choices.

Herein, we provide evidence that one of the two subgroups of MDS patients can achieve a more favorable clinical response to BCL2 inhibition by venetoclax-based therapy. Our preliminary data reveal that MCL1 is one of the determinants of venetoclax resistance in MDS patients and that combining MCL1 inhibition and venetoclax can synergistically eradicate venetoclax-resistant MDS blasts and HSPCs *in vitro* and reduce tumor burden in patient-derived xenografts. Additionally, in patients enrolled in clinical trials of venetoclax, we observed an expansion of a subset of CD4⁺ T cells with naïve and/or early-activated antigen-experienced phenotype only when the patients responded to venetoclax-based therapy, indicating a possible role of the adaptive immune system in mediating venetoclax response. This study substantiates the reliability of MDS patient stratification based on their immunophenotype in the clinical use of venetoclax-based therapy and assesses the feasibility of targeting MCL1 in venetoclax-resistant MDS patients as a novel therapeutic option to improve their survival.

TABLE OF CONTENTS

APPROVAL.....	I
TITLE	II
ACKNOWLEDGEMENTS	IV
ABSTRACT	VI
LIST OF TABLES.....	X
LIST OF FIGURES.....	XI
CHAPTER 1: INTRODUCTION	1
1.1 Myelodysplastic Syndromes (MDS) and the Hematopoietic Hierarchy	2
1.1.1 Overview	2
1.1.2 The Hematopoietic Hierarchy	2
1.1.3 Clonal Hematopoiesis and Genetics of MDS	4
1.2 The Standard of Care for MDS	6
1.2 Novel Stratification of MDS and its Clinical Implications.....	6
1.3.1 “CMP Pattern” and “GMP Pattern” MDS.....	6
1.3.2 Progression of MDS is Associated with the Immunophenotypically-defined HSPC Hierarchy.....	8
1.3 Apoptosis and BCL2 Family Proteins	11
1.4.1 BCL2 Family Proteins Mediate the Intrinsic Apoptosis Pathway	11
1.4.2 Targeting Anti-apoptotic Mechanisms with BH3 Mimetics	11
1.4.3 Venetoclax (ABT-199) and AMG-176	12
1.5 The Biology and Development of T Lymphocytes	13

CHAPTER 2: HYPOTHESIS AND SPECIFIC AIMS	15
CHAPTER 3: MATERIALS AND METHODS	18
CHAPTER 4: RESULTS	29
4.1 “CMP pattern” MDS Patients Can Achieve More Favorable Outcomes in Response to the Venetoclax-Based Therapy than “GMP Pattern” MDS Patients	30
4.2 Single-cell RNA Sequencing (scRNA-seq) Analyses Revealed the Potential Mechanisms of Venetoclax Resistance and Response in MDS Patients	32
4.2.1 Results from a representative “CMP pattern” MDS patient (P1)	32
4.2.2 Results from a representative “GMP pattern” MDS patient (P2)	37
4.3 Mass Cytometry Analysis (CyTOF) Validated the Results of scRNA-seq Analysis at Protein Level	42
4.3.1 Results from a representative “CMP pattern” MDS patient (P3)	42
4.3.2 Results from representative “GMP pattern” MDS patients (P2, P4).	43
4.4. T Cell Analyses by Flow Cytometry	48
4.5 Assessing the Feasibility of Targeting MCL1 in Venetoclax-Resistant MDS	55
4.5.1 The combination of venetoclax and AMG-176 can synergistically eradicate MDS-L cells <i>in vitro</i>	55
4.5.2 The combination of venetoclax and AMG-176 can synergistically suppress MDS stem cell survival <i>in vitro</i>	58
4.5.3 The combination of venetoclax and AMG-176 can significantly decrease BM chimerism in a “GMP pattern” MDS patient-derived xenograft (PDX).	60
CHAPTER 5: DISCUSSION	63

REFERENCES.....	69
VITA	82

LIST OF TABLES

Table 1. Immunophenotypic HSPC definitions used in the quantification and purification of human HSPCs by flow cytometry.....	20
Table 2. Immune cell definitions used in the quantification of human NK cells and T cells by flow cytometry	21
Table 3. List of antibodies used for CyTOF analysis panel for BM MNCs from MDS patients.	28

LIST OF FIGURES

Figure 1. Human adult hematopoiesis	3
Figure 2. Schematic of clonal hematopoiesis and propagation of hematologic malignancies.....	5
Figure 3. MDS are maintained by distinct and recurrent cellular hierarchies.....	10
Figure 4. Clinical outcomes of “CMP pattern” and “GMP pattern” MDS patients in response to venetoclax-based therapy.....	31
Figure 5. Flow cytometry plots of HSPCs in BM MNCs isolated from a representative “CMP pattern” MDS patient with <i>TP53</i> and <i>U2AF2</i> mutations	33
Figure 6. Single-cell RNA sequencing (scRNA-seq) analysis in Lin-CD34 ⁺ HSPCs isolated from sequential BM samples of a representative “CMP pattern” MDS patient.....	34
Figure 7. Single-cell RNA (scRNA-seq) sequencing analysis in BM MNCs isolated from the sequential BM samples of a representative “CMP pattern” MDS patient (P1)	36
Figure 8. BCL2 expression and <i>TP53</i> mutations are mutually exclusive.	37
Figure 9. Flow cytometry plots of HSPCs in BM MNCs isolated from sequential BM samples from a representative “GMP pattern” MDS patient (P2).....	39
Figure 10. Single-cell RNA (scRNA-seq) sequencing analysis in BM MNCs isolated from the sequential BM samples from a representative “GMP pattern” MDS patient (P2).....	42
Figure 11. Cytometry by time of flight (CyTOF) analysis of BM MNCs isolated from sequential BM samples from a representative “CMP pattern” MDS patient (P3).	44
Figure 12. Cytometry by time of flight (CyTOF) analysis in BM MNCs isolated from sequential BM samples of a representative “GMP pattern” MDS patient (P2).	46
Figure 13. Cytometry by time of flight (CyTOF) analysis in BM MNCs isolated from the sequential BM samples from a representative “GMP pattern” MDS patient (P4).....	47
Figure 14. T and NK cell quantification by flow cytometry.	49
Figure 15. CD4 ⁺ T cell quantification in BM MNCs by flow cytometry.....	50
Figure 16. CD4 ⁺ T cell quantification in the CD4 ⁺ T cell compartment by flow cytometry.....	51

Figure 17. CD4 ⁺ T cell quantification in sequential patient samples by flow cytometry	52
Figure 18. CD8 ⁺ T cell quantification in BM MNCS by flow cytometry.	53
Figure 19. CD8 ⁺ T cell quantification in the CD8 ⁺ compartment by flow cytometry.....	54
Figure 20. Effect of single-agent treatments with venetoclax (ABT-199) and AMG-176 on MDS-L cells.....	56
Figure 21. Apoptosis analysis and quantification in MDS-L cells after treatment with venetoclax (ABT-199) and AMG-176, as single agents and in combination.	57
Figure 22. Effect of single-agent and combination treatments with venetoclax (ABT-199) and AMG-176 in primary MDS HSCs.....	59
Figure 23. Effect of single-agent and combination treatments with venetoclax (ABT-199) and AMG-176 on a representative “GMP pattern” MDS patient-derived xenograft model (PDX).61	

CHAPTER 1: INTRODUCTION

1.1 Myelodysplastic Syndromes (MDS) and the Hematopoietic Hierarchy

1.1.1 Overview

Myelodysplastic syndromes (MDS) are a group of heterogeneous clonal hematopoietic disorders characterized by ineffective and dysplastic hematopoiesis [1]. Clinically, MDS patients display symptoms such as peripheral blood cytopenia, bone marrow hyperplasia, dysplasia, and a high risk of progression to acute myeloid leukemia [2]. In recent years, a dramatic increase in MDS incidence due to the aging of the population and increased cases of therapy-related MDS in cancer survivors has emphasized the importance of developing therapies to improve the survival of MDS patients [3].

1.1.2 The Hematopoietic Hierarchy

The key to understanding the pathology and progression of MDS is to investigate the mechanisms that regulate hematopoiesis and its functional dynamics. Hematopoiesis is a process that gives rise to all types of blood cells, which is governed by hematopoietic stem cells (HSCs) that reside in the bone marrow and possess the ability of self-renewal and differentiating into downstream progenitor cells [4]. The hierarchy of hematopoiesis was initially defined as the differentiation of HSCs as a discrete process based on early studies in mice [5, 6]. As the investigation of hematopoiesis has incorporated high-throughput single-cell transcriptomic analyses, the hierarchy of hematopoiesis has been supplemented with the identification of new HSC populations and the expansion of the complexity of lineage differentiation [7]. More importantly, these single-cell technologies have led to the current interpretation of hematopoietic hierarchy as a continuum process in which lineage specification is defined by the cells' transcriptional state, which mostly depends on transcription factor dynamics [8].

In humans, the long-term hematopoietic stem cells (LT-HSCs), which reside at the top of the hierarchy in the HSC compartment, represent a very rare population among cells in the bone marrow and proliferate mostly under conditions of stress [9]. They produce multipotent progenitors (MPPs), which frequently undergo differentiation into myeloid-biased common myeloid progenitors (CMPs), and lymphoid-biased lymphoid-primed multipotent progenitors (LMPPs). CMPs then differentiate into megakaryocyte/erythrocyte progenitors (MEPs) and granulocyte/monocyte progenitors (GMPs), while LMPPs give rise to common lymphoid progenitors (CLPs) (**Figure 1**) [9]. The progenitor cells further differentiate into more committed downstream blood cells that enter circulation in the body bearing distinct functions [9].

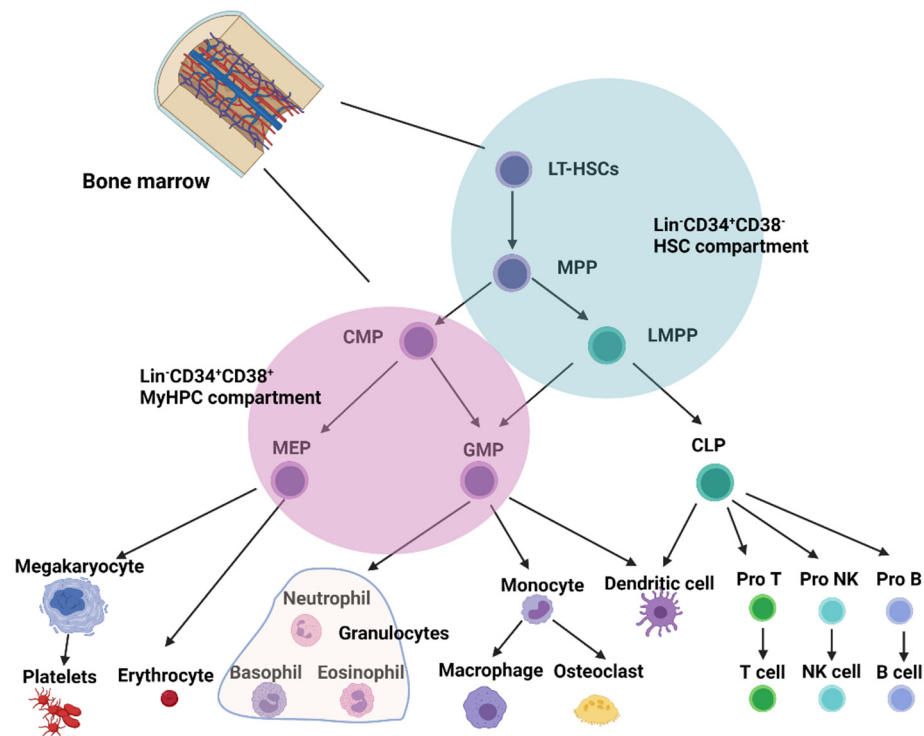


Figure 1. Human adult hematopoiesis

HSCs reside in the bone marrow and possess lifelong self-renewal and differentiation potential. Within the Lin⁻CD34⁺CD38⁻ HSC compartment, there are long-term hematopoietic stem cells (LT-HSCs), multipotent progenitors (MPPs), and lymphoid-primed multipotent progenitors

(LMPPs). Cells in the HSC compartment give rise to downstream progenitor populations, including megakaryocyte/erythrocyte progenitors (MEPs), common myeloid progenitors (CMPs), granulocyte/monocyte progenitors (GMPs), and common lymphoid progenitors (CLPs). CMPs are able to generate MEPs and GMPs for further maturation and differentiation of the myeloid lineages; MEPs further generates megakaryocytes and erythrocytes; GMPs differentiate into granulocytes, monocytes, and dendritic cells. CLPs mostly give rise to the lymphoid lineages, including T cells, natural killer (NK) cells, and B cells.

1.1.3 Clonal Hematopoiesis and Genetics of MDS

During aging, HSCs can acquire cumulative genetic alterations such as chromosomal aberrations and/or somatic mutations that confer survival advantages to the mutant cells over their normal counterparts [10-13]. Initially, these mutations can start by affecting only small populations of bone marrow cells, a process known as clonal hematopoiesis of indeterminate potential (CHIP). Over time, once additional disease-driving mutations occur, or under pressure from other external factors such as inflammation or chemotherapy [14], these CHIP clones can expand and evolve into MDS. MDS can then eventually progress to AML, mostly after therapy failure, when MDS clones acquire secondary mutations or undergo clonal evolution [11, 14-16].

Figure 2 summarizes the initiation and progression of MDS [17].

In the past two decades, the application of advanced genomic technologies has dramatically improved our understanding of the driver mutations associated with the positive selection of MDS clones. Early studies on the genetics of MDS focusing on cytogenetic abnormalities have revealed that about 50% of MDS patients have chromosomal and copy-number abnormalities (CNAs), of which the most frequent are -7 or del(7q) and -5 or del(5q) [18]. Additionally, recurrent somatic mutations in various functional pathways such as DNA methylation, chromatin/histone modification, splicing, and transcription have been identified in MDS [19, 20]. Mutations in genes that regulate epigenetic programs are the most frequently

observed, including mutations in *TET2*, *DNMT3A*, and *IDH1/2*, involved in DNA methylation; *ASXL1*, *MLL2*, and *EZH2*, involved in chromatin/histone modification; and *SF3B1*, *SRSF2*, and *U2AF1*, involved in RNA splicing regulation [21]. These mutant proteins play essential roles in hematopoiesis as they regulate the expression of genes that are fundamental for HSC self-renewal and differentiation [22].

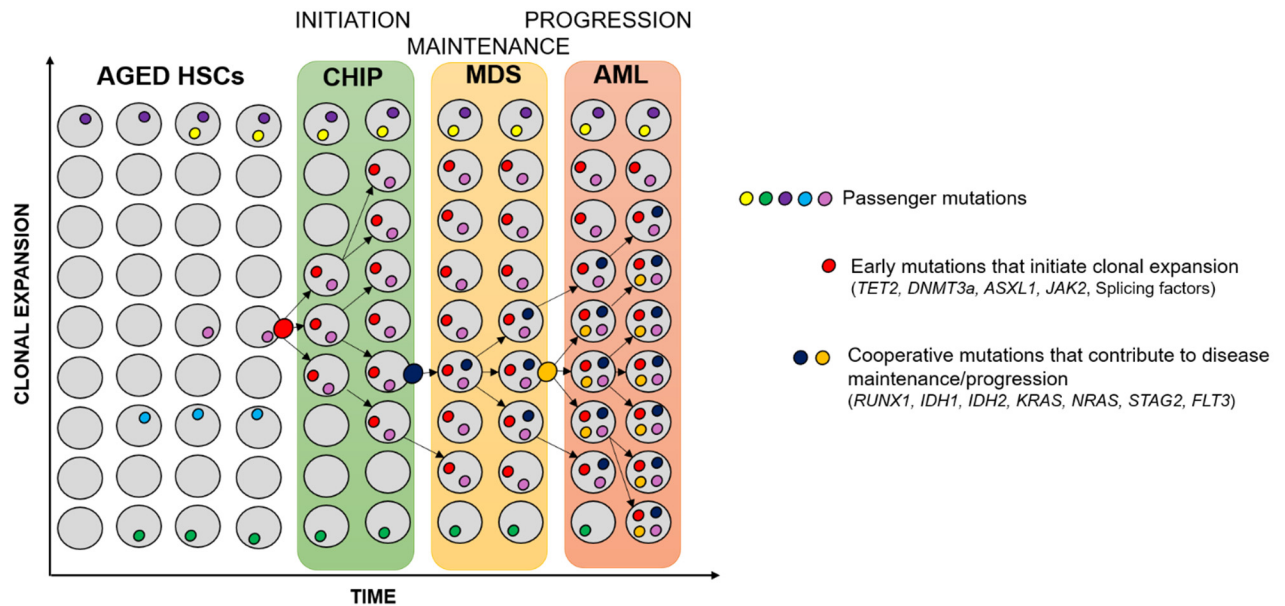


Figure 2. Schematic of clonal hematopoiesis and propagation of hematologic malignancies.

Early mutations (indicated as red circles) in hematopoietic stem cells (HSCs) initiate clonal hematopoiesis of indeterminate potential (CHIP). As HSCs acquire more disease-driving mutations (indicated as blue and orange circles), CHIP can progress to myelodysplastic syndromes (MDS) and eventually acute myeloid leukemia (AML). The figure is adapted from Steensma et al. *Blood* 2015 [17].

1.2 The Standard of Care for MDS

The current standard of care for MDS patients is hypomethylating agent (HMA)-based therapy using 5'-azacitidine or decitabine, which partially restores functional hematopoiesis, improves overall survival, and delays progression to AML compared to conventional therapy [23, 24]. The exact mechanisms and molecular targets of HMAs in MDS are unclear. Since anomalous epigenetic regulation is one of the consequences of recurrent somatic mutations in MDS, tumor suppressor genes that are crucial in regulating DNA damage, differentiation, and transcription might be silenced due to DNA hypermethylation mediated by DNA methyltransferases (DNMTs) [25]. 5-azacytidine and decitabine are examples of clinically effective HMAs that work by incorporating into DNA to target DNMTs for degradation, potentially inducing DNA hypomethylation and restoring gene transcription [26, 27]. However, the precise mechanisms involved in the direct association of DNMT inhibition and induction of DNA hypomethylation remain ambiguous [28].

In MDS, only 40-50% of the patients respond to HMA therapy with a transient response of 6 to 24 months. HMA treatment failure is usually followed by a poor prognosis and disease progression [29]. The only curative treatment for MDS is stem cell transplantation (SCT). However, not all MDS patients are eligible because of age and comorbidities [30]. Thus, MDS patients with HMA failure who are not eligible for SCT are in urgent need of effective second-line treatment options to improve their outcomes.

1.2 Novel Stratification of MDS and its Clinical Implications

1.3.1 “CMP Pattern” and “GMP Pattern” MDS

In order to provide MDS patients with more effective, precise, and personalized treatment, researchers have put enormous effort on elucidating a precise stratification of MDS patients over time. The gold standard for clinical risk assessment in MDS patients are the

International Prognostic Scoring System (IPSS) and Revised International Prognostic Scoring System (IPSS-R) that classify patients based on their blast count and the number of cytogenetic abnormalities and cytopenias [31]. However, although there have been significant refinements of the stratification and prognostication of MDS patients, both the IPSS and IPSS-R are limited to a particular group of patients and lack a base in molecular pathology [32].

Our lab has previously demonstrated that MDS patients can be stratified into two immunophenotypically and biologically distinct entities based on the bone marrow (BM) HSPC hierarchy. Specifically, we characterized the immunophenotypic profile of the HSPC compartment in a cohort of 123 BM samples isolated from untreated MDS patients. Unsupervised hierarchical clustering based on the frequency of immunophenotypically defined HSPC populations followed by principal component analysis stratified the MDS samples into two main groups. Compared with BM samples from age-matched healthy donors, the BM samples of one of the MDS groups (52% of the samples) had an abnormal differentiation pattern characterized by an increased frequency of CMPs within the myeloid hematopoietic progenitor cell (MyHPC) compartment (a “CMP pattern” of differentiation) owing to significantly decreased frequencies of GMPs and MEPs in the total BM mononuclear cells (MNCs). In contrast, the BM samples of the other MDS group (48% of the samples) had a higher frequency of GMPs within the MyHPC compartment (a “GMP pattern” of differentiation) owing to significantly decreased frequencies of CMPs and MEPs in the total BM MNCs. These 2 different MDS patterns were associated with distinct mutational landscapes that accounted for these subtypes’ different HSPC hierarchies. Specifically, we found that mutations in *RUNX1*, *BCOR*, *STAG2*, and *DNMT3A* were significantly more prevalent in “GMP pattern” MDS, whereas mutations in *TP53* and *U2AF1* were associated with the “CMP pattern” phenotype.

The immunophenotypic compositions of the 2 MDS subgroups’ upstream HSC precursors were significantly different. Specifically, whereas “CMP pattern” MDS samples had higher frequencies of LT-HSCs and MPPs, “GMP pattern” MDS samples had a significantly

higher frequency of LMPPs. These distinct HSC architectures arose from a significant expansion of the LMPPs in “GMP pattern” MDS in the context of an overall decrease in the frequencies of LT-HSCs and MPPs in total BM MNCs (**Figure 3**).

1.3.2 Progression of MDS is Associated with the Immunophenotypically-defined HSPC Hierarchy

In our study we also sought to elucidate the biological mechanisms underpinning blast progression (BP) in the two MDS groups, as such an understanding might lead to the development of new therapeutic approaches to prevent or overcome HMA failure. Given that HMA failure is mostly independent of the molecular and genetic alterations in the founder clone [33] and that BP is mostly associated with the expansion of HSC clones carrying preexisting or newly acquired recurrent mutations in genes involved in signal transduction and transcriptional and epigenetic regulation [16, 34, 35], we hypothesized that HSC expansion can be induced by key oncogenic pathways that are recurrently activated in each MDS group. To test this hypothesis, we evaluated gene expression changes in LT-HSC and LMPP populations isolated from “CMP pattern” and “GMP pattern” MDS patients, respectively, whose disease had become resistant to HMA therapy and progressed to higher-risk disease or AML.

RNA-seq analysis revealed that, compared with those isolated from untreated patients, LT-HSCs isolated from “CMP pattern” MDS patients with BP following HMA therapy failure had significantly upregulated genes involved in promoting cell proliferation and survival, including the anti-apoptotic regulator B-cell lymphoma 2 (*BCL2*). In striking contrast to our findings in “CMP pattern” MDS, genes involved in the tumor necrosis factor alpha (TNF α)-induced nuclear factor-kappa B (NF- κ B) signaling pathway were significantly upregulated in the LMPPs from “GMP pattern” MDS patients with BP as compared with LMPPs from “GMP pattern” MDS patients with newly diagnosed disease. These results have led to the hypothesis that “CMP pattern” MDS patients with BP may benefit from BCL2 inhibition and “GMP pattern” patients

with BP may benefit from NF- κ B inhibition. Indeed, our most exciting finding was that the pharmacological inhibition of either of these pathways selectively depletes the respective MDS stem cell types *in vitro* and decreases tumor burden in patient-derived xenograft models. On the basis of these results, we hypothesized that targeting BCL2 with venetoclax elicits a durable response in “CMP pattern” MDS, potentially providing a means of improving patient stratification in clinical trials of this drug. These results have led to clinical trials of venetoclax-based therapy in MDS patients following HMA failure at MD Anderson Cancer Center.

In this Thesis, I sought to understand the mechanisms that contribute to venetoclax response and resistance by analyzing sequential BM samples isolated from MDS patients enrolled in prospective clinical trials and identify novel therapeutic targets that can overcome venetoclax resistance in order to improve the survival and prognosis of MDS patients effectively. Given that the upregulation of myeloid cell leukemia 1 (*MCL1*) is one of the mechanisms of resistance to venetoclax identified among AML patients and can be upregulated downstream by NF- κ B [36, 37], we hypothesized that MCL1 inhibition, alone or in combination with venetoclax, can effectively target MDS at progression in patients who failed HMA therapy alone or in combination with venetoclax. Indeed, recent pre-clinical studies in chronic lymphocytic leukemia (CLL) and AML have shown the synergistic effect of BCL2 and MCL1 inhibition in suppressing the growth of blasts and leukemogenic stem cells [38-40]. However, whether this combination will have an effect in MDS has not been elucidated.

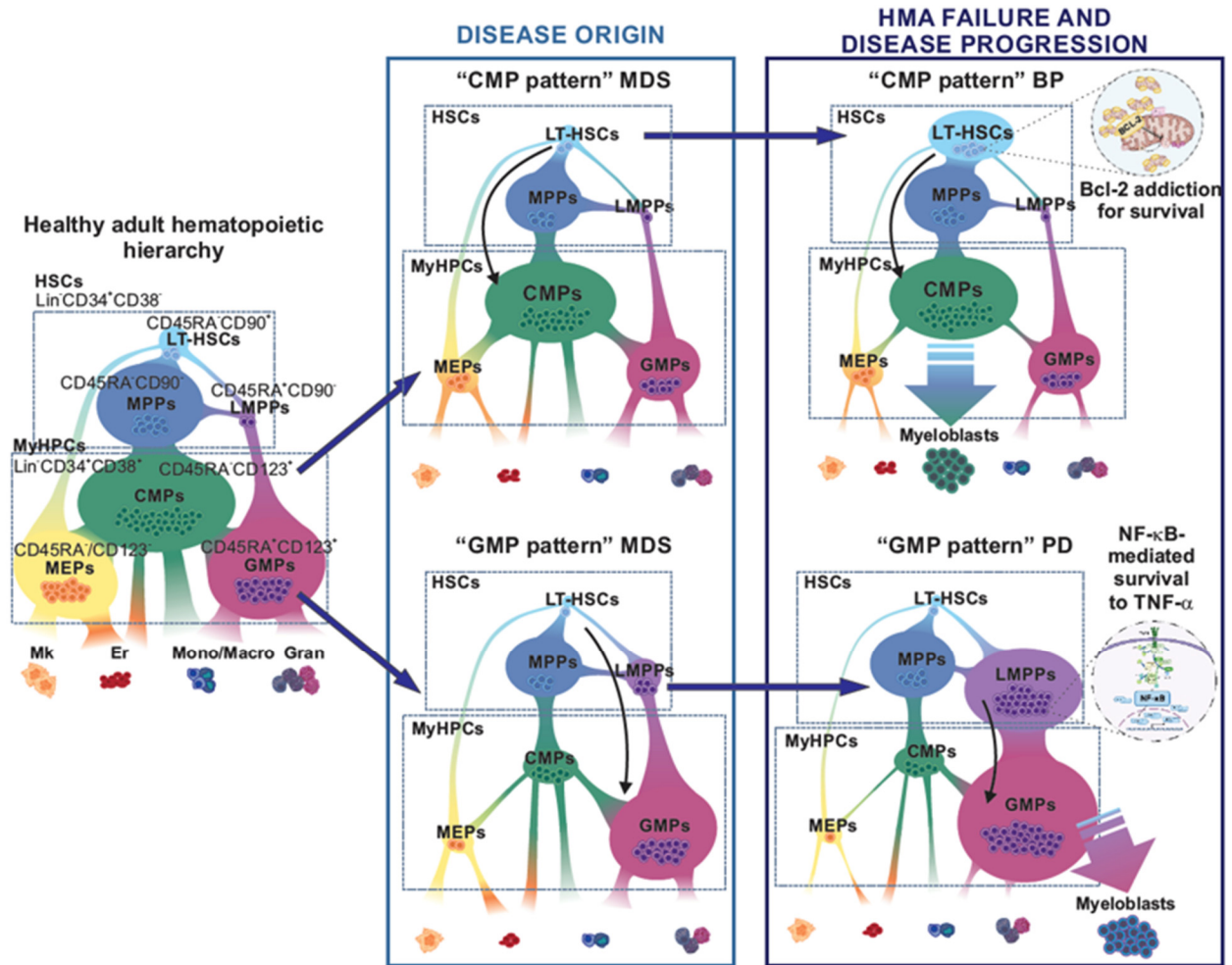


Figure 3. MDS are maintained by distinct and recurrent cellular hierarchies.

Previous findings by Ganan-Gomez *et al.* demonstrated that MDS patients can be stratified into two immunophenotypically and biologically distinct entities based on the hematopoietic stem and progenitor cell (HSPC) hierarchy. Long-term hematopoietic stem cells (LT-HSCs) rely on BCL2 upregulation for survival and drive disease progression in the "CMP pattern" MDS. Lymphoid-primed multipotent progenitors (LMPPs) upregulate NF-κB signaling pathways for survival and drive disease progression in the "GMP pattern" MDS. Figure taken from Ganan-Gomez *et al.* (under revision in *Nature*).

1.3 Apoptosis and BCL2 Family Proteins

1.4.1 BCL2 Family Proteins Mediate the Intrinsic Apoptosis Pathway

To maintain homeostasis, human bodies require programmed cell death to remove damaged or dysfunctional cells that disrupt normal physiology and tissue functions. Apoptosis is one of the conserved and regulated mechanisms of programmed cell death orchestrated by both extrinsic and intrinsic signaling pathways [41]. Composed of both pro-survival and pro-apoptotic members, BCL2 family proteins mediate the intrinsic apoptosis pathway by triggering mitochondrial outer membrane permeabilization (MOMP). Following MOMP, the subsequent release of cytochrome *c* from the mitochondria is activated by pro-apoptotic BCL2 family members (BAX, BAK1, BIM, BID, and PUMA), which can be antagonized by the anti-apoptotic BCL2 family members (BCL2, BCL-XL, BCL-W, BCL2-A1, and MCL1). Each member in this family has at least one of the four BCL2 homology (BH) domains (BH1-BH4). The pro-apoptotic family members are the BH3-only proteins (BIM, BID, NOXA, BIK, PUMA, BMF, and HRK) which, as the name indicates, contain only the BH3 domain. They bind to anti-apoptotic members and consequently unleash BAX/BAK and initiate apoptosis through MOMP. As a result, cytochrome *c* is released into the cytoplasm, leading to the formation of apoptosome and downstream caspase signaling activation [42-44].

1.4.2 Targeting Anti-apoptotic Mechanisms with BH3 Mimetics

Resistance to cell death is one of the hallmarks of cancer [45]. One of the mechanisms contributing to the evasion of apoptosis in cancer cells is the upregulation of the expression of pro-survival members of the BCL2 protein family. Indeed, the overexpressed pro-survival members sequester the pro-apoptotic members, preventing them from activating MOMP [43]. The identification of this anti-apoptotic mechanism in multiple cancer types, along with insightful studies on the structural interactions between pro-survival and pro-apoptotic members, has led

to the development of small molecule drugs called “BH3 mimetics” that are designed to mimic the binding of BH3-only BCL2 family members to pro-survival members. Since BH3 mimetics are engineered to have a much higher binding affinity to the pro-survival BCL2 family proteins than the actual BH3-only proteins, they are capable of disrupting protein-protein interactions between BH3-only proteins and pro-survival proteins, such that the BH3-only proteins are set free to initiate apoptosis [46].

1.4.3 Venetoclax (ABT-199) and AMG-176

Re-engineered from navitoclax (ABT-263), which was the first orally available BH3 mimetic, venetoclax (ABT-199) is a selective BCL2 inhibitor. First reported in 2013 [47], venetoclax has demonstrated great anti-neoplastic effectiveness as a single agent or in combination with approved cancer therapies in preclinical/clinical studies for various cancer types, leading to the FDA approval of venetoclax in combination with other therapies as a treatment for CLL patients with 17p deletion in 2016 [48] and for newly-diagnosed AML patients in 2018 [49]. Unlike navitoclax, ABT-199 had less binding affinity to BCL-X_L, which is critical for platelet survival in order to prevent thrombocytopenia [47].

Although venetoclax treatment has greatly improved the survival of patients with hematologic malignancies, primary or secondary resistance to venetoclax can eventually occur. MCL1 is one of the pro-survival members of BCL2 family proteins whose upregulation has been identified as one of the mechanisms of venetoclax resistance [50-52]. These findings have led to the development of the BH3 mimetics S63845, S64315/MIK665, AMG176 and AZD5991, each targeting MCL1 activity [40, 53, 54]. AMG-176 was first reported by Caenepeel *et al.* in 2018 as a novel orally bioavailable MCL1 inhibitor that could induce tumor cell apoptosis in multiple myeloma xenografts and have significant synergistic effect on killing AML cells *in vivo* in combination with venetoclax treatment [53]. Thus, in our pre-clinical study, we

utilized AMG-176 to evaluate the efficiency of MCL1 inhibition, as monotherapy or in combination with venetoclax, in overcoming venetoclax resistance.

Moreover, recent studies have linked venetoclax response to T lymphocyte activities in which venetoclax could lead to an increase in intratumoral CD8⁺ memory T cells, potentially enhancing the anti-tumor immune response when combined with immunotherapy [55]. Thus, besides the direct targeting of venetoclax to BCL2-expressing cancer cells, venetoclax may also induce an anti-tumor adaptive immune response by augmenting T lymphocytes' cytotoxicity [56].

1.5 The Biology and Development of T Lymphocytes

Our immune system is composed of various immune cells that are responsible for recognizing and fighting non-self pathogens. The engagement of the immune system in cancer patients has become a central focus for understanding the complexity dynamics and interactions among cancer cells, tumor microenvironment, and cancer therapeutics. The T lymphocyte in particular, with its capacity for antigen-directed cytotoxicity, exhibits a great potential for application in cancer immunotherapy and vaccinology, and has led to extensive study of its biology and development [57].

The progenitors of T cells originate in the BM and then migrate to the thymus and initiate T cell development. Early committed T cells are termed “double-negative” T cells owing to their lack of CD4 and CD8 T cell receptor (TCR) expression. Once they are able to successfully express CD4 and CD8 pre-TCRs, they will transit to double-positive T cells and further, depending on their binding ability and affinity to either MHC I complex or MHC II complex during positive and negative selections, become single-positive (SP) T cells with the expression of either CD4 or CD8 [58]. Within each SP subset, there are various T cell subpopulations that have been identified with distinct functions. These include the following: naïve T cells (T_N, CD45RA⁺CD45RO⁻CD95⁻CCR7⁺⁺), stem-cell-like memory T cells (T_{SCM},

CD45RA⁺CD45RO⁻CD95⁺CCR7⁺), effector T cells (T_E, CD45RA⁺CD45RO⁻CD95⁺CCR7⁻), central memory T cells (T_{CM}, CD45RA⁻CD45RO⁺CD95⁺CCR7⁺), effector memory T cells (T_{EM}, CD45RA⁻CD45RO⁺CD95⁺CCR7⁻), and regulatory T cells (T_{reg}, CD4⁺CD25⁺FOXP3⁺CD127^{lo}). Following antigen recognition, naïve T cells become activated and develop the ability to differentiate into multiple memory T cell subsets. T_{SCM} is the subset that has come across antigen; however, it maintains a naïve-like phenotype in which it is able to sustain its self-renewal ability and reconstitute the full spectrum of memory and effector T cells [59]. More committed memory T cells are composed of T_{CM} and T_{EM}, distinguished based on the presence and absence of surface lymph node homing receptor CD62L (L-selectin) and C-C chemokine receptor 7 (CCR7) [60]. The memory T cell subsets are the key to the sustainability of long-term immunity as they recognize and respond to the re-stimulation of previously exposed antigens and differentiate into T_E to launch cytotoxic activities [61, 62]. Lastly, T_{reg} is an immunosuppressive CD4⁺ T cell subset that maintains tolerance to self-antigens through the downregulation of effector T cell activities to prevent autoimmune diseases [63].

T cell are key mediators in immune surveillance and anti-tumor activities. Recent studies have reported significant population changes in T cells in response to venetoclax treatment in cancer patients [55, 56]. In this Thesis, I also sought to understand whether T cell-mediated immunity could potentially play a part in venetoclax response in MDS.

CHAPTER 2: HYPOTHESIS AND SPECIFIC AIMS

Based on our previous studies, we hypothesized that “CMP pattern” MDS patients can achieve favorable clinical outcomes in response to BCL2 inhibition by venetoclax-based therapy. In addition, since MCL1 upregulation is a potential determinant of venetoclax resistance in AML [52] and *MCL1* is the downstream target of NF- κ B pathway activation [64], we also hypothesized that MCL1 inhibition, alone or in combination with venetoclax can effectively overcome venetoclax resistance in MDS.

To test our hypotheses, I pursued the following two specific aims:

Aim #1. Identify predictive biomarkers of venetoclax response and resistance by analyzing sequential BM samples from MDS patients enrolled in prospective clinical trials

1a. Test the hypothesis that venetoclax-based therapy can selectively eradicate “CMP pattern” MDS HSCs.

To achieve this aim, I evaluated the correlation between the 2 MDS HSPC architectures and the clinical response to venetoclax-based therapy.

1b. Dissect molecular determinants of venetoclax response and resistance in different cell types.

To achieve this aim, I performed scRNA-seq analysis of BM MNCs and Lin⁻CD34⁺ HSPCs from sequential BM samples isolated from patients enrolled in the venetoclax-based clinical trials at different therapy time points (before therapy, and at the times of remission, stable disease, and progression).

1c. Evaluate whether venetoclax response, resistance, or failure is associated with the differential expression of key anti-apoptotic proteins.

To achieve this aim, I performed cytometry by time-of-flight (CyTOF) analysis of BM MNCs isolated from sequential BM samples isolated from patients enrolled in the venetoclax-based clinical trials at different therapy time points (as defined in aim 1b).

1d. Evaluate whether the adaptive immune system plays a role in mediating the response to venetoclax-based therapy.

To achieve this aim, I evaluated whether venetoclax-based therapy induces immunophenotypic changes in composition of the T and NK cell compartments.

Aim #2. Assess the feasibility of targeting MCL1 in patients with venetoclax-resistant MDS.

2a. Evaluate whether AMG-176 alone or in combination with venetoclax can eradicate venetoclax-resistant blasts and HSPCs in vitro.

To achieve this aim, I treated the MDS cell line MDS-L and primary samples from patients with MDS at the time of progression, in co-culture with mesenchymal cells, with AMG-176 alone or in combination with venetoclax.

2b. Evaluate whether AMG-176 can eradicate venetoclax-resistant tumor burden in vivo.

To achieve this aim, I treated patient-derived xenografts with AMG-176 alone or in combination with venetoclax.

CHAPTER 3: MATERIALS AND METHODS

Human primary samples and cell lines. BM specimens from 35 patients who were diagnosed with MDS or secondary AML and referred to the Department of Leukemia at MD Anderson Cancer Center were obtained with the approval of the Institutional Review Board and in accordance with the Declaration of Helsinki. Written informed consent was obtained from all donors, and all MDS diagnoses were confirmed by dedicated hematopathologists. Responses to therapy in patients enrolled in clinical trials were assessed by dedicated hematologists. BM MNCs were isolated from each sample using the standard gradient separation approach with Ficoll-Paque PLUS (GE Healthcare Lifesciences, Pittsburgh, PA). For cell sorting applications, MNCs were enriched in CD34⁺ cells using magnetic sorting with the CD34 Microbead Kit (Miltenyi Biotec, San Diego, CA) and further purified by flow cytometric sorting as described below. For transplantation purposes, CD3⁺ cells were depleted from the BM MNCs by using magnetic sorting with the CD3 Microbead Kit (Miltenyi Biotec, San Diego, CA). Human BM-derived mesenchymal stromal cells (MSCs) were obtained from healthy BM donors as previously described [65] and kindly provided by Dr. Michael Andreeff from the Department of Leukemia at MD Anderson. The MDS-L cell line was kindly donated by Dr. Kaoru Tohyama (Department of Laboratory Medicine, Kawasaki Medical School, Okayama, Japan). The identity of the MDS-L line was confirmed by short tandem repeat DNA fingerprinting at MD Anderson's Characterized Cell Line Core Facility.

Flow cytometry and fluorescence-activated cell sorting. Quantitative flow cytometric analyses and fluorescence-activated cell sorting (FACS) of human live MNCs and CD34⁺ cells were performed using previously described staining protocols [13, 66] and antibodies against CD2 (RPA- 82.10), CD3 (SK7), CD14 (MφP9), CD19 (SJ25C1), CD20 (2H7), CD34 (581), CD56 (B159), CD71 (M-A712), CD123 (9F5), and CD235a (HIR2; all from BD Biosciences); CD4 (S3.5), CD11b (ICRF44), CD33 (P67.6), CD45RA (MEM-56), and CD90 (5E10; all from Thermo Fisher Scientific); CD7 (6B7), CD38 (HIT2), and CD135 (6H6; all from BioLegend, San

Diego, CA); and CD10 (SJ5-1B4; Leinco Technologies, St Louis, MO). Stem and progenitor cell populations were classified using published definitions [67-69]. Detailed information about the flow cytometry and FACS settings and the antibody panels used to identify specific HSPC populations is provided in **Table 1**.

POPULATION	GATING STRATEGY
LIVE CELLS	Single cells/Sytox Green Nucleic Acid Stain negative (Thermo Fisher Scientific)
LINEAGE NEGATIVE CELLS (LIN⁻)	CD2 ⁻ , CD3 ⁻ , CD4 ⁻ , CD7 ⁻ , CD10 ⁻ , CD11b ⁻ , CD14 ⁻ , CD19 ⁻ , CD20 ⁻ , CD33 ⁻ , CD56 ⁻ , CD235a ⁻
HSC COMPARTMENT	Live/Lin ⁻ /CD34 ⁺ , CD38 ⁻
LT-HSCs	Live/Lin ⁻ /CD34 ⁺ , CD38 ⁻ /CD90 ⁺ , CD45RA ⁻
MPPs	Live/Lin ⁻ /CD34 ⁺ , CD38 ⁻ /CD90 ⁻ , CD45RA ⁻
LMPPs	Live/Lin ⁻ /CD34 ⁺ , CD38 ⁻ /CD90 ⁻ , CD45RA ⁺
MyHPC COMPARTMENT	Live/Lin ⁻ /CD34 ⁺ , CD38 ⁺
CMFs	Live/Lin ⁻ /CD34 ⁺ , CD38 ⁺ /CD123 ⁺ , CD45RA ⁻
GMPs	Live/Lin ⁻ /CD34 ⁺ , CD38 ⁺ /CD123 ⁺ , CD45RA ⁺
MEPs	Live/Lin ⁻ /CD34 ⁺ , CD38 ⁺ /CD123 ⁻ , CD45RA ⁻

Table 1. Immunophenotypic HSPC definitions used in the quantification and purification of human HSPCs by flow cytometry

Abbreviations: HSPC, hematopoietic stem and progenitor cell; HSC, hematopoietic stem cell; LT-HSCs, long-term HSCs; MPPs, multipotent progenitors; LMPPs, lymphoid-primed MPPs; MyHPC, myeloid hematopoietic progenitor cell; CMFs, common myeloid progenitors, GMPs, granulocyte-monocyte progenitors; MEPs, megakaryocyte-erythroid progenitors.

In patient-derived xenograft mice, human chimerism was analyzed by staining the mouse BM suspensions, prepared as described above, with antibodies against human CD45 (clone HI30) and mouse CD45 (clone 30-F11; both from BioLegend).

For immune cell analysis, BM MNCs were stained with antibodies against CD56 (5.1H11), CD16 (3G8), CD3 (UCHT1), CD4 (RPA-T4), CD8 (SK1), CD45RO (UCHL1),

CD45RA (HI100), CD197 (G043H7), CD95 (DX2), CD25 (BC96), CD127 (A019D5), and FOXP3 (206D; all from BioLegend). Detailed information about the flow cytometry and FACS settings and the antigen panels used to identify specific immune cell populations is provided in

Table 2.

POPULATION	GATING STRATEGY
LIVE CELLS	Single cells/ Zombie UV™ Fixable Viability negative (BioLegend)
NK CELLS	Live CD3 ⁺ CD56 ⁺ CD16 ^{hi/lo}
T CELLS	Live CD3 ⁺ CD56 ⁻ CD4 ⁺ and Live CD3 ⁺ CD56 ⁻ CD8 ⁺
T_N	Live/CD3 ⁺ CD56 ⁻ CD4 ⁺ /CD45RA ⁺ CD45RO ⁻ CD95 ⁻ CCR7 ⁺⁺ and Live/CD3 ⁺ CD56 ⁻ CD8 ⁺ /CD45RA ⁺ CD45RO ⁻ CD95 ⁻ CCR7 ⁺⁺
T_{SCM}	Live/CD3 ⁺ CD56 ⁻ CD4 ⁺ /CD45RA ⁺ CD45RO ⁻ CD95 ⁺ CCR7 ⁺ and Live/CD3 ⁺ CD56 ⁻ CD8 ⁺ /CD45RA ⁺ CD45RO ⁻ CD95 ⁺ CCR7 ⁺
T_{CM}	Live/CD3 ⁺ CD56 ⁻ CD4 ⁺ /CD45RA ⁻ CD45RO ⁺ CD95 ⁺ CCR7 ⁺ and Live/CD3 ⁺ CD56 ⁻ CD8 ⁺ /CD45RA ⁻ CD45RO ⁺ CD95 ⁺ CCR7 ⁺
T_{EM}	Live/CD3 ⁺ CD56 ⁻ CD4 ⁺ /CD45RA ⁻ CD45RO ⁺ CD95 ⁺ CCR7 ⁻ and Live/CD3 ⁺ CD56 ⁻ CD8 ⁺ /CD45RA ⁻ CD45RO ⁺ CD95 ⁺ CCR7 ⁻
T_E	Live/CD3 ⁺ CD56 ⁻ CD4 ⁺ /CD45RA ⁺ CD45RO ⁻ CD95 ⁺ CCR7 ⁻ and Live/CD3 ⁺ CD56 ⁻ CD8 ⁺ /CD45RA ⁺ CD45RO ⁻ CD95 ⁺ CCR7 ⁻
T_{reg}	Live/CD3 ⁺ CD56 ⁻ CD4 ⁺ CD25 ⁺ FOXP3 ⁺ CD127 ^{lo}

Table 2. Immune cell definitions used in the quantification of human NK cells and T cells by flow cytometry

Abbreviations: NK, natural killer; T_N, naïve T cells; T_{SCM}, stem cell memory T cells; T_{CM}, central memory T cells; T_{EM}, effector memory T cells; T_E, terminal effector T cells; T_{reg}: regulatory T cells.

For Annexin V/DAPI apoptosis analysis, MDS-L cells were incubated with fluorochrome-conjugated Annexin V (Miltenyi Biotec, San Diego, CA) in 1X binding buffer for 10-15 minutes at RT in the dark. Then cells were washed with binding buffer and resuspended in 4',6-Diamidino-2-Phenylindole, Dihydrochloride (DAPI) solution.

Samples used for flow cytometry and FACS were acquired with a BD LSR Fortessa or BD Influx Cell Sorter (BD Biosciences), and the cell populations were analyzed using FlowJo

software. All experiments included fluorescence-minus-one and single-stained controls and were performed at MD Anderson's South Campus Flow Cytometry & Cell Sorting Core Facility.

Western blots. Cells were washed with a 10% fetal bovine serum (FBS)/phosphate-buffered saline (PBS) solution (FBS/PBS) and pellets were resuspended in Mammalian Cell & Tissue Extraction Kit buffer (BioVision Incorporated, Milpitas, CA) and incubated for 15 minutes with gentle shaking. Lysates were then collected after centrifugation for 20 minutes at 12,000 rpm and 4°C. The amount of protein was quantified using the Qubit™ Protein Assay Kit and a Qubit fluorometer (both from Thermo Fisher Scientific). Sodium dodecyl sulfate–polyacrylamide gel electrophoresis and Western blotting were performed following standard protocols. Blotted membranes were incubated with primary monoclonal antibodies against human BCL2 (clone 124, Dako), MCL1 (Cell Signaling Technology, Danvers, MA), and vinculin (clone hVIN-1, Sigma-Aldrich) and with secondary anti-mouse and anti-rabbit digital antibodies (Kindle Biosciences LLP, Durham, NC). Membranes were developed using the SuperSignal™ West Pico PLUS Chemiluminescent Substrate (Thermo Fisher Scientific) in a KwikQuant Imager (Kindle Biosciences LLP).

Immune cell staining. BM MNC pellets were washed with PBS and incubated with Zombie UV™ Fixable Viability dye (BioLegend, San Diego, CA) in PBS for 15 minutes at room temperature (RT) and in the dark. After incubation, cells were washed with thawing buffer (50% FBS, 25% NaCl solution, and 25% anticoagulant solution) and were stained with 11 antibodies against surface markers as described below, for 40 minutes at 4°C and in the dark. After staining, cells were washed with thawing buffer and incubated with 1x Fix solution from the TruNuclear Transcription Factor Buffer Set (BioLegend) for 1 hour at 4°C in the dark. When the incubation was finished, cells were washed three times with 1x permeabilization buffer and stained with an intracellular antibody against FOXP3 as described below, for 45 minutes at RT

and in the dark. After the intracellular staining, cells were washed with permeabilization buffer and then with thawing buffer. They were then resuspended in 350 μ L of 2% FBS/PBS and transferred to flow cytometry tubes for cytometric analysis as described below.

Patient-derived xenograft mouse models. Mice were maintained under specific-pathogen-free conditions at MD Anderson mouse facility. All animal experiments were performed with the approval of MD Anderson's Institutional Animal Care and Use Committee. All animal studies used 5-week-old mice unless otherwise indicated. NSGS (NSG-SGM3) mice were purchased from the Jackson Laboratory (Bar Harbor, ME). NSG-SGM3 mice were sub-lethally irradiated and were injected with 0.5×10^6 patient-derived CD3⁻ BM MNCs. Engraftment was periodically assessed by determining the human CD45 chimerism rate by flow cytometric analysis of BM aspirates as described above. If chimerism analysis indicated that there was significant engraftment of human cells, mice were randomized into four groups: control, ABT-199, AMG-176, and their combination. For ABT-199 treatment, mice were treated with 50mg/kg/day of ABT-199 daily by oral gavage for two weeks and/or with 30 mg/kg/day of AMG-176 treatment on the first two days of the week for two weeks. At the end of the treatment, the mice were sacrificed and autopsied, and their rear legs were resected for analysis. For BM flow cytometric analyses, femurs and tibias were crushed in the presence of a 2% FBS/PBS solution, the cell suspensions were passed through 30 μ m pre-separation filters (Miltenyi Biotec), and the cells were counted to assess BM cellularity. BM cells were stained with fluorochrome-conjugated antibodies as described below.

Drugs and treatments. ABT-199 was provided by AbbVie (North Chicago, IL). For *in vitro* experiments, ABT-199 was dissolved in DMSO and diluted in PBS. For *in vivo* experiments, fresh suspensions of ABT-199 in a 60:30:10 mix of Phosal 50 PG (Lipoid, Newark, NJ), polyethylene glycol (PEG) 400, and ethanol were prepared weekly and stored at +4°C. ABT-

199 was administered by gavage at a dose of 50 mg/kg/day. AMG-176 was provided by Amgen (Thousand Oaks, CA). For *in vitro* experiments, AMG-176 was dissolved in DMSO and diluted in PBS. For *in vivo* experiments, fresh suspensions of AMG-176 in 25% hydroxypropyl beta cyclodextrin with NaOH were sonicated for 2 hours at 60°C (pH=9), which were prepared weekly and stored at RT. Mice were given 30 mg/kg daily on the first two days of the week for two weeks by oral gavage.

Histological analyses. All human BM biopsy specimens (core biopsy specimens) were routinely collected and processed in MD Anderson's Department of Hematopathology. BM biopsy specimens were fixed in 10% neutral buffered formaldehyde, and core biopsy specimens were further decalcified using 10% formic acid for 3 h at 50°C in a microwave processor. Specimens were embedded in paraffin, and 4 µm sections were prepared for antibody detection. Immunohistochemistry (IHC) was performed at the Dana Farber/Harvard Cancer Center Specialized Histopathology Core (Boston, MA). Formalin-fixed paraffin-embedded samples were stained with anti-human BCL2 (clone 124; Dako, Agilent, Santa Clara, CA) and counterstained with hematoxylin.

scRNA-seq. For scRNA-seq, BM samples were first processed and enriched as described above, and 3,000 Lin⁻CD34⁺ cells were sorted by FACS. Sample preparation and sequencing were performed at MD Anderson's Sequencing and Microarray Facility. Sample concentration and cell suspension viability were evaluated using a Countess II FL Automated Cell Counter (Thermo Fisher Scientific) and manual counting. Samples were normalized for input onto the Chromium Single Cell A Chip Kit (10x Genomics, Pleasanton, CA), in which single cells were lysed and barcoded for reverse-transcription. The pooled single-stranded, barcoded cDNA was amplified and fragmented for library preparation. During library preparation, appropriate

sequence primer sites and adapters were added for sequencing on a NextSeq 500 sequencer (Illumina).

After sequencing, fastq files were generated using the cellranger mkfastq pipeline (version 3.0.2). The raw reads were mapped to the human reference genome (refdata-cellranger-GRCh38-3.0.0) using the cellranger count pipeline. The digital expression matrix was extracted from the filtered_feature_bc_matrix folder outputted by the cellranger count pipeline. Multiple samples were aggregated using the cellranger aggr pipeline. The digital expression matrix was analyzed with the R package Seurat (version 3.0.2) [70] to identify different cell types and signature genes for each. Cells with fewer than 500 unique molecular identifiers or greater than 50% mitochondrial expression were removed from further analysis. The Seurat function NormalizeData was used to normalize the raw counts. Variable genes were identified using the FindVariableFeatures function. The ScaleData function was used to scale and center expression values in the dataset, and the number of unique molecular identifiers was regressed against each gene. PCA, tSNE, and uniform manifold approximation and projection (UMAP) were used to reduce the dimensions of the data, and the first two dimensions were used in the plots. The FindClusters function was used to cluster the cells. Marker genes for each cluster were identified using the FindAllMarkers function. Cell types were annotated based on the marker genes and their match to canonical markers.

CyTOF analysis. The CyTOF panel was modified from the AML panel that Dr. Andreeff established previously to include MDS HSPC markers. Briefly, sequential samples will be stained with a CyTOF panel that includes 52 antibodies against lineage markers (e.g., CD45, CD11b, CD4, CD8a, CD3, CD68, CD56, CD123, CD34, CD45RA, CD38, CD19, CD33, CD90, HLA-DR, and HLA-ABC), BCL2 family proteins (i.e., BCL2, MCL1, PUMA, NOXA, BIM, BCL-X_L, BAD, and BAX), and proteins involved in signaling pathways (e.g., p-p65, p-4EBP1, p-STAT5, p-GSK, p-STAT3, pS6, p-ERK, p-MEK1/2, p-AKT, and p-FLT3). To minimize variability in

antibody staining and instrument sensitivity, the Cell-ID 20-Plex Pd barcoding kit was used.

This kit is ideal for barcoding clinical trial samples collected longitudinally and enables batched samples collected at different times to be run simultaneously (up to 20 per run) [71]. ViSNE [72] was used to analyze patients' longitudinal data, which enabled us to characterize the BM cell populations within each sample, track the way in which the composition of these populations shifts before and after drug treatment, and identify the characteristics of vulnerable and drug-resistant populations.

AML Panel 1		AML Panel 2		AML Panel 3		T- CELL	
Isotope	Antigen	Isotope	Antigen	Isotope	Antigen	Isotope	Antigen
89	CD45	89	CD45	89	CD45	89	CD45
102	CD45	102	CD45	102	CD45	102	CD45
103	CD45	103	CD45	103	CD45	103	CD45
104	CD45	104	CD45	104	CD45	104	CD45
105	CD45	105	CD45	105	CD45	105	CD45
106	CD45	106	CD45	106	CD45	106	CD45
108	CD45	108	CD45	108	CD45	108	CD45
110	CD45 (All CD45 for barcoding)	110	CD45	110	CD45	110	CD45
111	CD11B	111	CD11B	111	CD45	111	CD45
112	CLA	112	CLA	112	CD45	112	CLA
113	CD8a	113	CD8a	113	CD8a	113	CD8
114	CD47	114	CD47	114	CD45	114	CD47
115	CD3	115	CD3	115	CD3	115	CD3
116	Cleaved PARP	116	Cleaved PARP	116	h2AX	116	Cleaved PARP
127	IDU	127	IDU	127	IDU	127	IDU
139	CD36	139	CD36	139	CD7	139	CD36
140	Ubiq	140	Ubiq	140	CD14	140	CD14
141	BCL-X _L	141	p- Rb(S807/S 811)	141	PTEN	141	ccr6
142	CD68	142	cleaved caspase	142	CD68	142	CD27
143	CD56	143	CD56	143	VDAC1	143	CD56
144	BCL2	144	p-Tyrosine	144	GOT2	144	CD26
145	CD123	145	CD123	145	CD71	145	NKG2A
146	BIM	146	BIM BD	146	CD64	146	CD49F

147	p-4EBP1(T37/46)	147	b-catenin	147	beta catenin	147	CD127
148	CD34	148	CD34	148	CD34	148	CCR2
149	BAD	149	p-NFKB	149	CD99	149	CCR4
150	p-Stat5(Y694)	150	SOD2	150	CD304	150	CD28
151	CLL-1	151	CLL-1	151	HES1	151	TBET
152	p-Stat3(Y705)	152	A1, Bfl-1	152	CD86	152	TIGIT
153	P21	153	BRD4	153	CD45RA	153	CD45RA
154	Ki-67	154	Ki-67	154	CD13	154	Ki-67
155	PDL1	155	PDL1	155	HIF1A	155	CCR7
156	CD38	156	CD38	156	P-p38(180/182)	156	TIM3
157	CD19	157	CD19	157	CD19	157	CD19
158	CD33	158	CD33	158	CD33	158	2B4
159	p-AKT	159	p-MAPKAPK-2	159	CD135	159	ICOS
160	Ythdf2	160	p27	160	ApoE 160Gd	160	PD-1
161	p-GSK-3 161Dy	161	nrf2	161	CytoC	161	CXCR3
162	Survivin	162	CDT1	162	CD120B	162	EOMES
163	C-myc	163	c-myc	163	Galectin-9	163	CD137
164	MDM2	164	p-AMPK	164	CD96	164	CTLA4
165	P53	165	p-creb	165	ABCB1	165	CD25
166	c-kit	166	C-kit	166	active B-catenin	166	LAG3
167	p-ERK	167	p-ERK	167	CD275	167	CXCR5
168	NOXA	168	MCT1	168	Mct1	168	CD160
169	p-MEK1/2	169	clpP	169	p-ENOS	169	CD69
170	Puma	170	ARC	170	IdH1	170	CD39
171	CD4	171	CD4	171	Bax	171	CD161
172	pS6	172	pS6	172	hnrpk	172	KLRG1
173	Bax	173	p-nrf2	173	CD70	173	CD95
174	p-FLT3	174	bcl2	174	CD200	174	GITR
175	CXCR4	175	cxcr4	175	p-FAK	175	CD4
176	Mcl-1	176	Cyclin B1	176	IRF4	176	CD38
194	CD15	194	CD15	194	CD15	194	CD57
195	HLA ABC	195	HLA ABC	195	CD66	195	HLA ABC

196	Live dead	196	Live dead	196	LD	196	Live Dead
198	HLA-DR	198	HLA-DR	198	CD4	198	HLA-DR
209	H3K27	209	IKBa	209	CD47	209	CD11b

Table 3. List of antibodies used for CyTOF analysis panel for BM MNCs from MDS patients.

Data analysis. Flow cytometry data and cell culture data were analyzed with Prism 8 software (GraphPad, La Jolla, CA). Figure legends indicate the statistical tests used in each experiment. For the analyses involving human samples, investigators were blinded to sample annotations and patient outcomes. Statistical significance was represented as *P<0.05, **P<0.01, ***P<0.001, ****P<0.0001.

CHAPTER 4: RESULTS

4.1 “CMP pattern” MDS Patients Can Achieve More Favorable Outcomes in Response to the Venetoclax-Based Therapy than “GMP Pattern” MDS Patients

To evaluate whether the immunophenotypic profile of MDS patients was associated with the clinical outcomes of venetoclax-based therapy, we analyzed the frequencies of HSPCs in total MNCs isolated from sequential BM samples of MDS patients enrolled in prospective venetoclax-based clinical trials. Preliminary clinical data showed that patients with “GMP pattern” MDS have a higher rate of disease progression without prior response than those with the “CMP pattern” MDS do (**Figure 4a**). These results suggested that the “CMP pattern” MDS patients could potentially achieve more favorable outcomes in response to the venetoclax-based therapy. However, these data were preliminary because most of the patients included in the analysis had received only a few cycles of therapy at the time of this Thesis submission. Moreover, flow cytometry analysis of HSPCs in sequential samples showed that LT-HSCs were depleted in the BM of “CMP pattern” MDS patients who responded to venetoclax-based therapy (**Figure 4b**), which is consistent with our lab’s previous finding that BCL2 inhibition by venetoclax could selectively eradicate disease-driving HSCs in patients with “CMP pattern” MDS. In contrast, LMPPs from “GMP pattern” MDS patients were not significantly affected during clinical responses (**Figure 4b**), suggesting that in “GMP pattern” MDS, the disease-driving stem cells did not rely on BCL2-mediated anti-apoptotic mechanisms for survival and disease propagation.

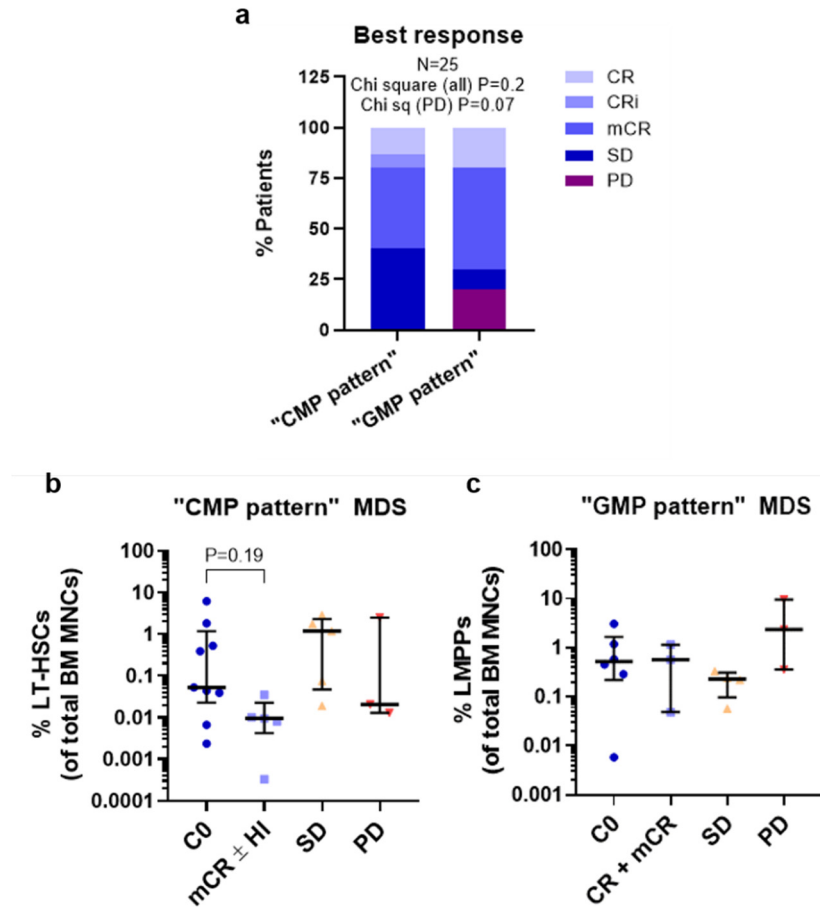


Figure 4. Clinical outcomes of “CMP pattern” and “GMP pattern” MDS patients in response to venetoclax-based therapy.

(a) Frequencies of complete remission (CR), complete remission with incomplete hematologic recovery (CRi), marrow complete remission (mCR), stable disease (SD), and progressive disease (PD) among 25 patients who received at least two cycles of venetoclax-based therapy (P=0.07 for PD between the 2 MDS groups; chi-square test). **(b)** Frequencies of LT-HSCs in the BM mononuclear cells (MNCs) of “CMP pattern” MDS patients at different times following venetoclax based therapy (P=0.19 between cycle 0 [C0] of venetoclax-based therapy after HMA therapy failure) and mCR; Wilcoxon matched pairs signed rank test. Only paired samples were analyzed). **(c)** Frequencies of LMPPs in the BM MNCs of “GMP pattern” MDS patients at different times after venetoclax based therapy.

4.2 Single-cell RNA Sequencing (scRNA-seq) Analyses Revealed the Potential Mechanisms of Venetoclax Resistance and Response in MDS Patients

4.2.1 Results from a representative “CMP pattern” MDS patient (P1)

To identify the potential molecular determinants of venetoclax response and resistance, we analyzed the transcriptomic changes induced by venetoclax-based therapy in BM HSPCs and MNCs isolated from sequential BM samples of two representative patients at the single-cell level. **Figure 5** shows the HSPC analysis of one of the patients with “CMP pattern” MDS (P1) with ringed sideroblasts and *TP53* and *U2AF2* mutations. This patient was enrolled in the clinical trial after HMA failure (Cycle 0 = C0). At time point C1, when the patient received one cycle of venetoclax-based therapy and achieved marrow complete remission (mCR), the proportion of HSC (Lin⁻CD34⁺CD38⁻) cells in BM MNCs as well as the frequency of LT-HSCs (Lin⁻CD34⁺CD38⁻CD90⁺CD45RA⁻) in the HSC compartment decreased compared to that at time point C0. However, the patient failed to respond to the second cycle of the therapy (C2) and entered a pre-relapse stage followed by disease progression at C3 (BM sample not available). Consistent with the clinical outcome, flow cytometry analysis showed that the BM frequency of the HSC compartment dramatically increased at C2 (**Figure 5**).

ScRNA-seq analysis of HSPCs isolated from the same sequential BM samples revealed that these cells underwent significant transcriptomic changes after the first cycle of venetoclax-based therapy (C1) when this patient achieved mCR compared with the time of enrollment (C0) (**Figure 6a, b**). Surprisingly, most HSPCs expressed *MCL1* but not *BCL2* (**Figure 6c, d**).

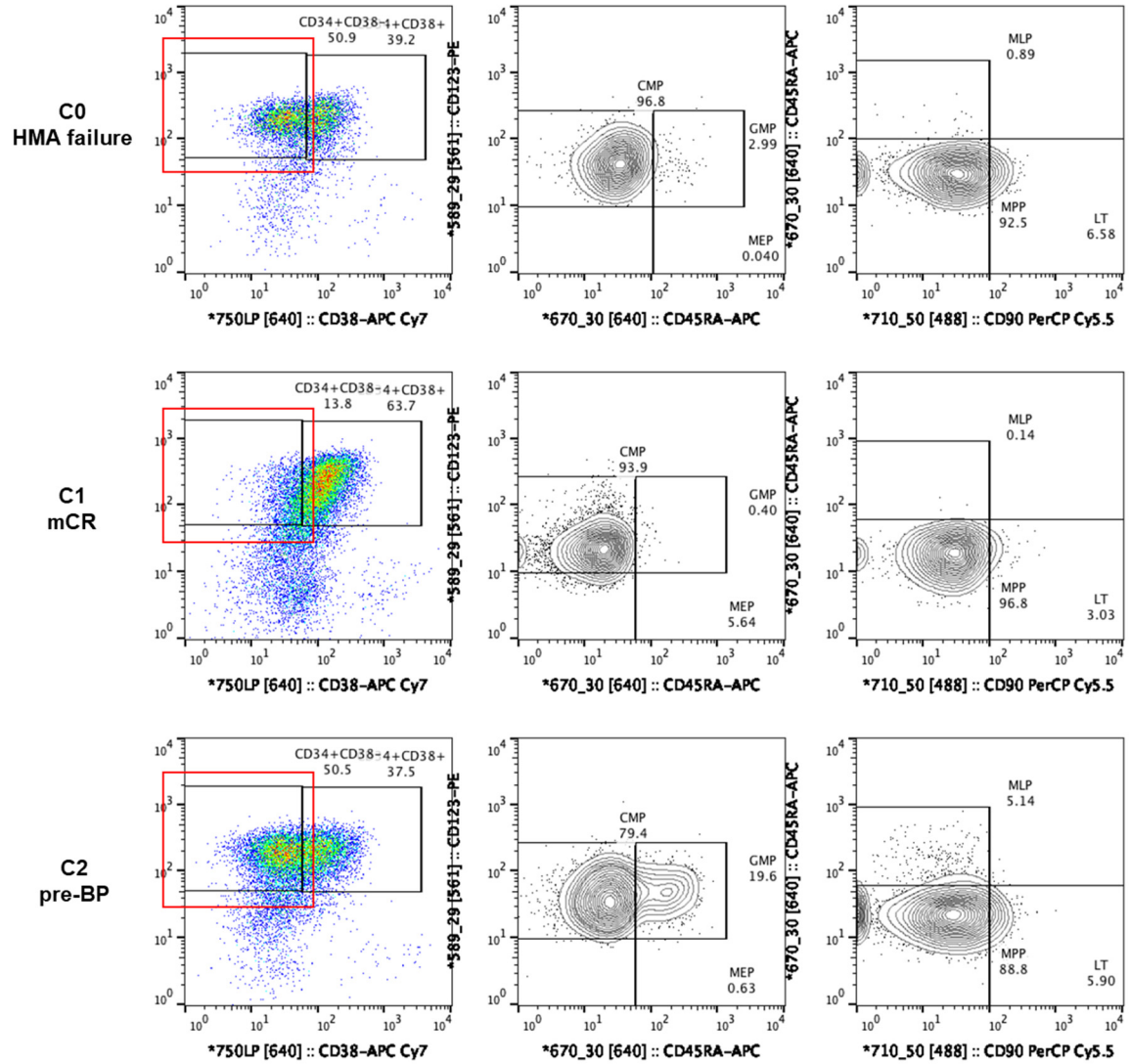


Figure 5. Flow cytometry plots of HSPCs in BM MNCs isolated from a representative “CMP pattern” MDS patient with *TP53* and *U2AF2* mutations

Patient P1 was enrolled in the clinical trial of venetoclax-based therapy after HMA therapy failure (C0). The patient had marrow complete remission (mCR) after the first cycle of therapy (C1) but had progression to AML after the second cycle (C2). Red squares indicate the Lin⁻ CD34⁺CD38⁻ population.

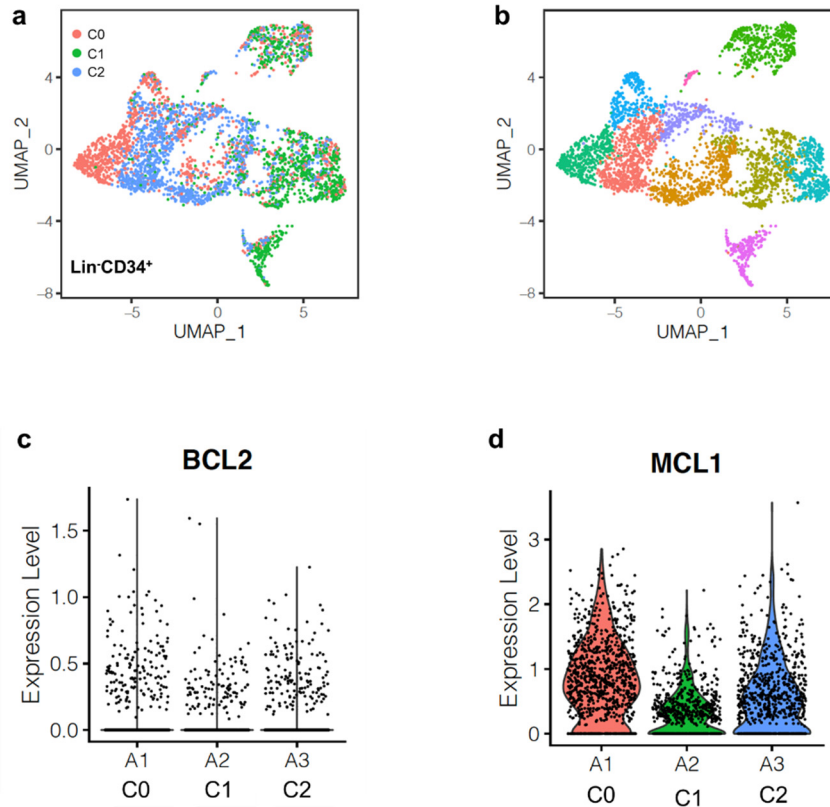


Figure 6. Single-cell RNA sequencing (scRNA-seq) analysis in Lin⁻CD34⁺ HSPCs isolated from sequential BM samples of a representative “CMP pattern” MDS patient

(a, b) Uniform manifold approximation and projection (UMAP) plots of single Lin⁻CD34⁺ HSPCs isolated from a patient with “CMP pattern” MDS at three different times after venetoclax based therapy and analyzed by scRNA-seq. Each dot represents one cell. The sample origin (a) and the cluster identity (b) of each cell are indicated by different colors. (c, d) Violin plots of *BCL2* (c) and *MCL1* expression (d) in the three samples.

ScRNA-seq analysis of total BM MNCs isolated from this patient (Figure 7a, b) revealed that, at C0 *BCL2* was only expressed in CD4⁺ T cells (Figure 7c) but not in the erythroid blasts. In addition, after the patient completed the first cycle of therapy and achieved mCR, CD4⁺ T cells were enriched within the T and NK cell compartments (Figure 7d).

Furthermore, the transcriptomic profile of the enriched CD4⁺ T cells suggested that they were naïve and/or early-activated antigen-experienced cells with expression of *CCR7*, *CD28*, and *CD27* (**Figure 7e**). Pathway enrichment analysis of genes differentially expressed in CD4⁺ T cells after venetoclax therapy compared with pre-treatment cells showed that venetoclax significantly upregulated genes involved in the oxidative phosphorylation pathway and the cytokine/inflammatory response (data not shown).

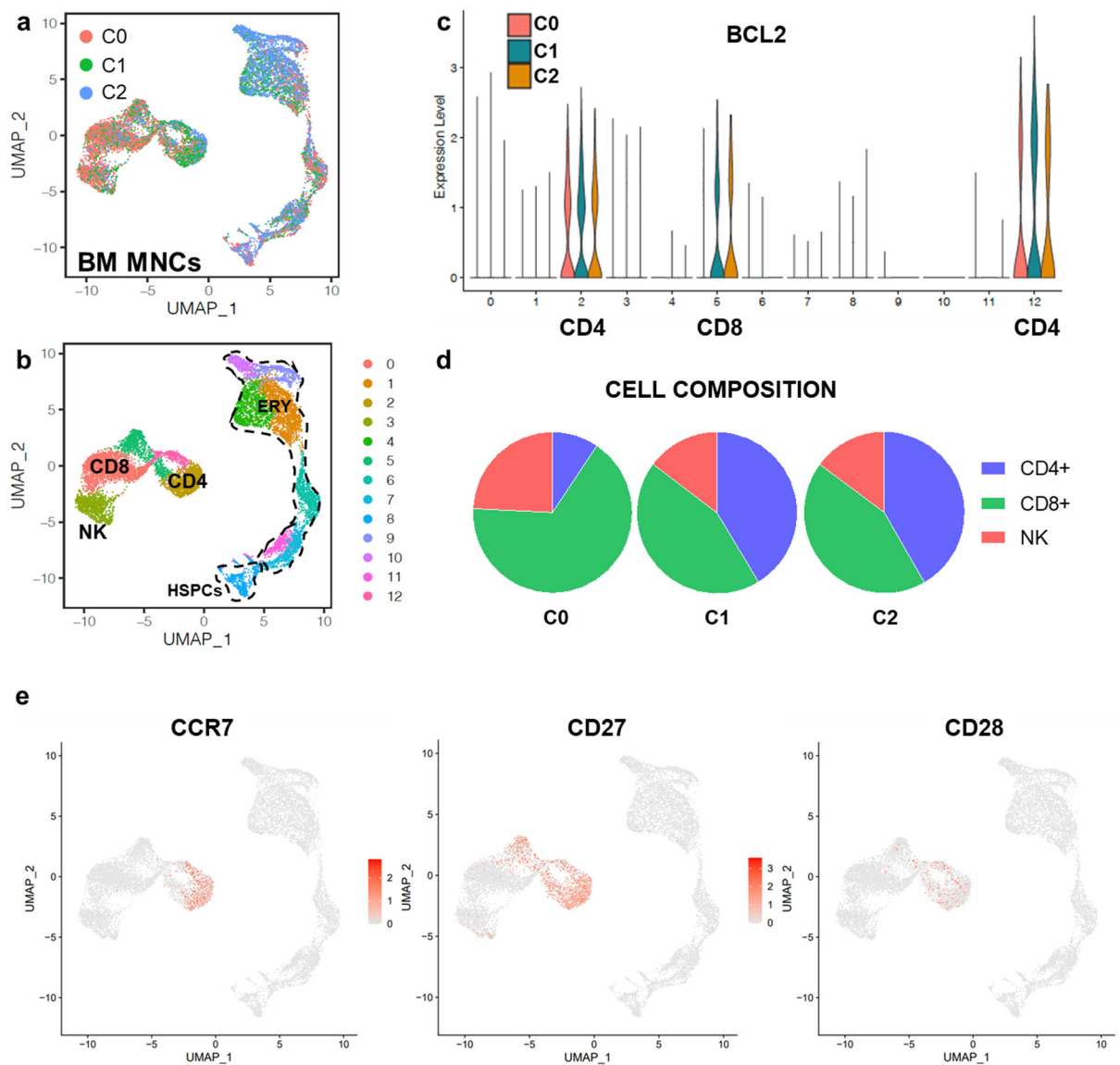


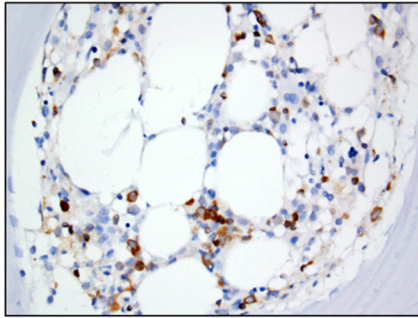
Figure 7. Single-cell RNA (scRNA-seq) sequencing analysis in BM MNCs isolated from the sequential BM samples of a representative “CMP pattern” MDS patient (P1)

(a, b) UMAPs of scRNA-seq data of single BM MNCs isolated from a patient with “CMP pattern” MDS at three different times during venetoclax-based therapy. Each dot represents one cell. Different colors indicate the sample origin **(a)** and the cluster identity **(b)** of each cell. **(c)** Violin plot of *BCL2* expression across the 13 MNC clusters. **(d)** Frequencies of CD4⁺ and CD8⁺ lymphocytes and natural killer (NK) cells in the T and NK compartments at different times of venetoclax-based therapy. HSPC, hematopoietic stem and progenitor cell; ERY, erythroid; NK, natural killer. **(e)** UMAP plots of *CCR7*, *CD27*, and *CD28* expressions among BM MNC clusters.

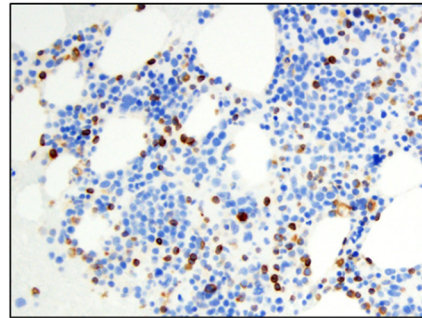
Together, these results suggest that the initial response to venetoclax-based therapy in this *TP53*-mutant patient was not mediated by targeting the HSPC and leukemic populations. It is therefore tempting to hypothesize that the initial response to therapy was mediated by an enhanced adaptive immune response. Of note, our immunohistochemistry analyses of *BCL2* expression in the blasts of BM biopsies from 2 MDS patients carrying *TP53* mutations after HMA therapy failure and 2 MDS patients with wild-type *TP53* (**Figure 8**), confirmed that *BCL2* expression and *TP53* mutations can be mutually exclusive in MDS.

***TP53* wild type**

UPIN#216

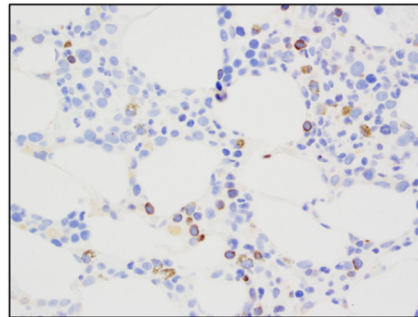


UPIN#042



***TP53* mutant**

UPIN#121



UPIN#050

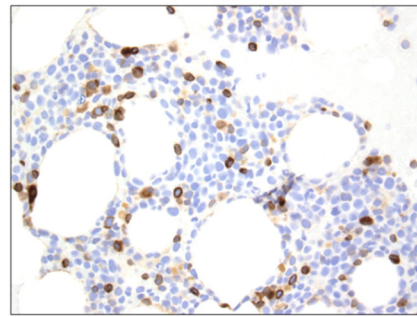


Figure 8. BCL2 expression and *TP53* mutations are mutually exclusive.

BM biopsy specimens from 4 representative “CMP pattern” MDS patients with wild-type or mutant *TP53* and progressive disease, stained with anti-human BCL2 antibody.

UPIN#216: *TP53* wild type with 5-10% CD34⁺ blasts; UPIN#042: *TP53* wild type with 6% CD34⁺ blasts; UPIN#121: *TP53* mutant with 15% CD34⁺ blasts; UPIN#050: *TP53* mutant with 41% CD34⁺ blasts, and 1% eosinophils which are positive for BCL2 staining regardless of the genetic background and here are considered false positives. Magnification is 400x.

4.2.2 Results from a representative “GMP pattern” MDS patient (P2).

Next, we analyzed by scRNA-seq sequential samples from a representative “GMP pattern” MDS patient (P2) with prior therapy failure and gene mutations in *ASXL1*, *TET2*, *RUNX1*, and *SRSF2*. Flow cytometry analyses of HSPCs in sequential BM samples from this

patient at five different times of therapy are shown in **Figure 9**: C0 (enrollment to the clinical trial after prior therapy failure), C2, C4, C7, and C8. Notably, the initial diagnosis of this patient was chronic myelomonocytic leukemia. When this patient relapsed after C8, the blastic cells were LMPPs instead of monoblasts and they represented the 17.6% of BM MNCs compared with the 0.26% at C0 (**Figure 9**). This is consistent with our previous findings that disease progression in “GMP pattern” MDS is driven by the expansion of LMPPs.

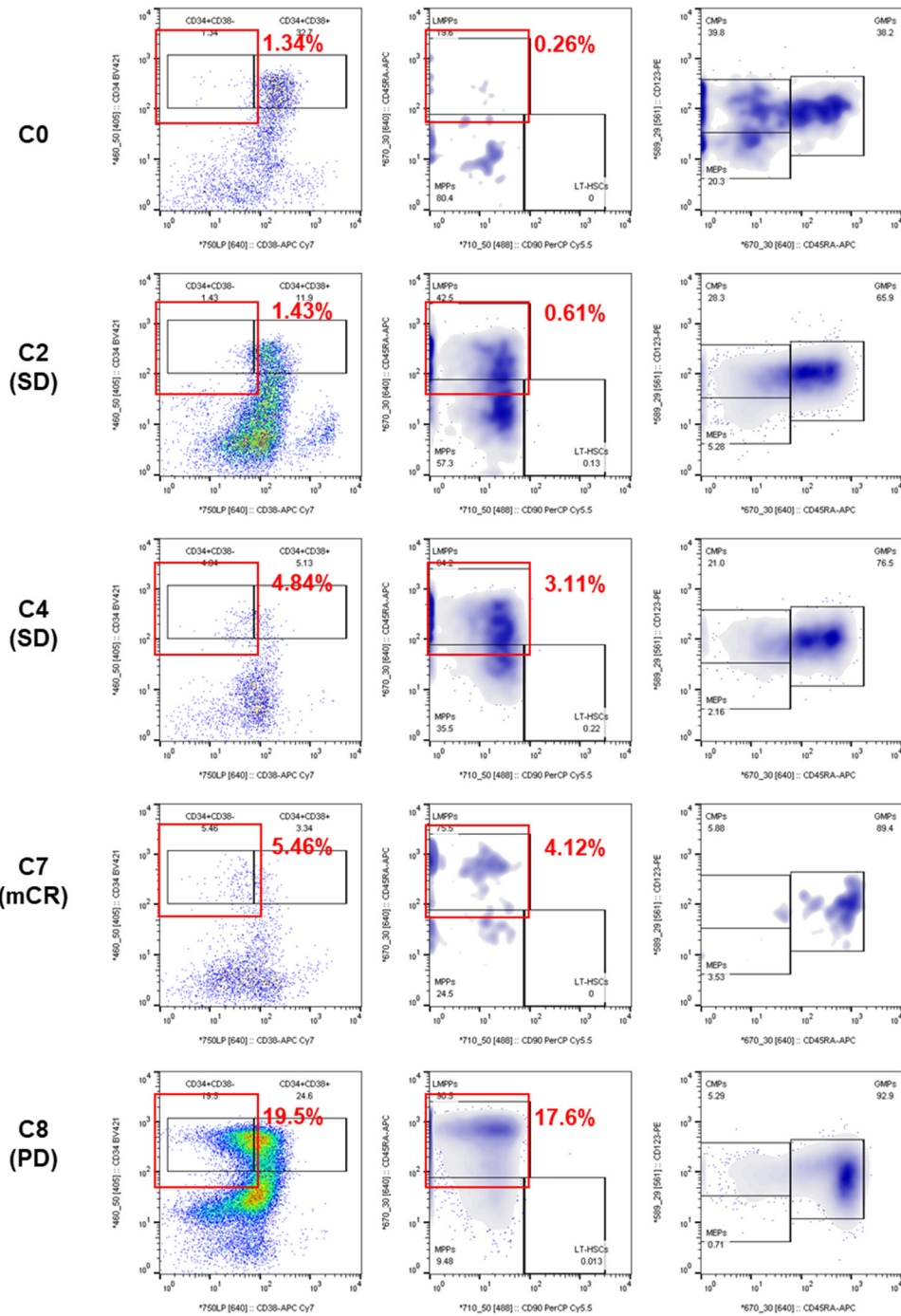


Figure 9. Flow cytometry plots of HSPCs in BM MNCs isolated from sequential BM samples from a representative “GMP pattern” MDS patient (P2).

Patient P2 was enrolled in the clinical trial of venetoclax-based therapy after HMA therapy failure (C0). The patient had marrow complete remission (mCR) after the second cycle of

therapy (C2), stable disease (SD) after the fourth cycle (C4), and mCR after the seventh cycle (C7), but had progression to AML (progressive disease, PD) after the eighth cycle (C8). The red squares indicate the Lin⁻CD34⁺CD38⁻ HSCs (first column) and LMPP populations (second column); numbers by the red squares represent the frequencies of HSCs in the Lin⁻CD34⁺ HSPC compartment (first column) and the frequencies of LMPPs in the Lin⁻CD34⁺CD38⁻ HSC compartment.

The transcriptomic profile of BM MNCs isolated from patient P2's sequential BM samples analyzed by scRNA-seq (**Figure 10a, b**) also showed that neither the monoblasts nor the LMPPs expressed *BCL2*, while *MCL1* was highly expressed in both (**Figure 10c, d**), suggesting that the direct cellular targets of venetoclax were not monoblasts or disease-driving LMPPs. Since *MCL1* can be upregulated by NF- κ B [64] and pathway enrichment analysis of LMPPs isolated from P2 at C8 (progressive disease, PD) demonstrated that the genes involved in the TNF α -induced NF- κ B signaling pathway were overexpressed in LMPPs after venetoclax-therapy failure (**Figure 10e**), the high expression of *MCL1* in P2's HSPCs might be due to the upregulation of the NF- κ B signaling pathway in LMPPs. This is consistent with our lab's previous finding that LMPPs of "GMP pattern" MDS patients with HMA failure are addicted to the NF- κ B-mediated signaling pathway for survival. Together with our finding that *MCL1*, but not *BCL2*, is upregulated in HSCs from "CMP pattern" patients with *TP53* mutations (**Figure 6, 7 and 8**), these results suggest that targeting *MCL1* may overcome venetoclax-based therapy resistance.

Similar to the observation in the "CMP Pattern" MDS patient analyzed by scRNA-seq (**Figure 8c**), *BCL2* was highly expressed in T cells (**Figure 10c**) and T cell population frequency changes also occurred when the patient achieved mCR during the venetoclax-based treatment. CD4⁺ T cells with a naïve and/or early-activated antigen-experienced phenotype

were enriched within the T and NK cell compartments when this patient underwent mCR

(Figure 10f).

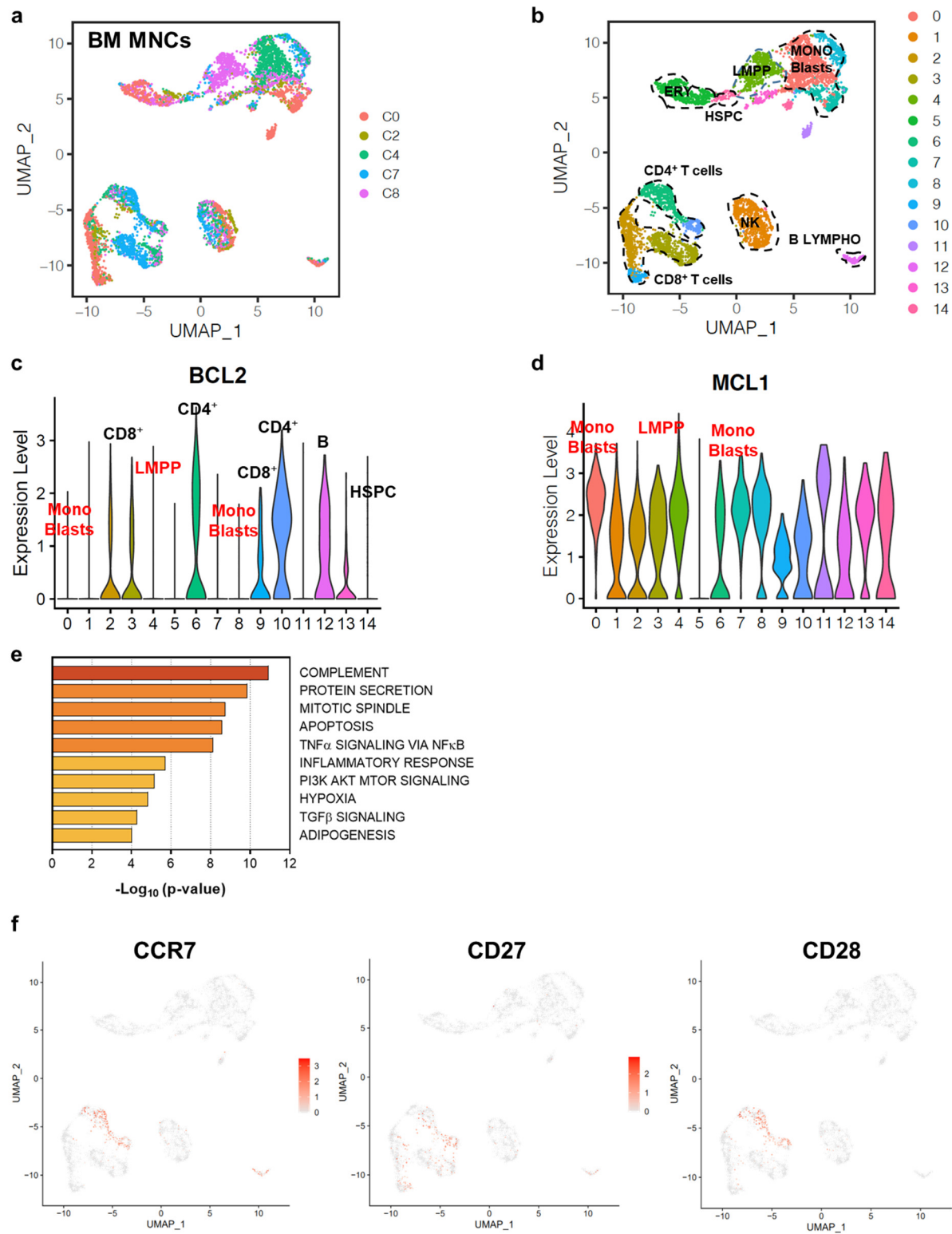


Figure 10. Single-cell RNA (scRNA-seq) sequencing analysis in BM MNCs isolated from the sequential BM samples from a representative “GMP pattern” MDS patient (P2).

(a, b) UMAP of scRNA-seq data of single BM MNCs cells isolated from a patient with “GMP pattern” MDS (P2) at five different times during venetoclax-based therapy. Each dot represents one cell. Different colors indicate the sample origin **(a)** and cluster identity **(b)** of each cell. **(c, d)** Violin plots of *BCL2* expression **(c)** and *MCL1* expression **(d)** across the 15 MNC clusters. HSPC, hematopoietic stem and progenitor cell; LMPP, lymphoid primed progenitors; ERY, erythroid; MONO, monocytic; LYMPHO, lymphoid; NK, natural killer. **(e)** Pathways significantly overexpressed in LMPPs at the time of disease progression after venetoclax-based therapy failure. **(f)** UMAP plots of *CCR7*, *CD27*, and *CD28* distributed among BM MNCs.

4.3 Mass Cytometry Analysis (CyTOF) Validated the Results of scRNA-seq Analysis at Protein Level

4.3.1 Results from a representative “CMP pattern” MDS patient (P3).

To investigate whether the outcomes of venetoclax-based therapy were associated with differential protein expression of critical anti-apoptotic BCL2 family proteins and to validate the findings obtained using scRNA-seq analysis, we employed CyTOF to analyze MNCs isolated from sequential BM samples from three additional MDS patients (P2, P3, and P4). **Figure 11** illustrates the CyTOF analysis results of 4 sequential BM MNC samples from a representative “CMP pattern” MDS patient with HMA failure and no *TP53* mutations (P3). The patient achieved mCR after C3 of venetoclax-based therapy but discontinued the therapy for reasons not related to the response and developed progressive disease. Unlike the MDS patient with *TP53* mutation shown in the previous section (**Figure 8**), this patient had high protein expression of BCL2 in the CD34⁺ HSPCs (**Figure 11a-c**). This results further confirmed our lab’s previous finding that “CMP pattern” MDS patients without *TP53* mutations acquire

upregulation of BCL2 expression in the disease-driving HSCs following HMA failure. The fact that the frequency of BCL2-expressing CD34⁺ HSPCs decreased before and at the time of marrow response to therapy (**Figure 11d**) also supports our hypothesis that BCL2 inhibition by venetoclax can selectively eradicate the disease-driving HSCs in “CMP pattern” MDS patients with HMA failure.

Additionally, as shown in **Figure 11d**, CD4⁺ T cells were also enriched in the BM MNCs when the patient responded to venetoclax-based therapy.

4.3.2 Results from representative “GMP pattern” MDS patients (P2, P4).

We next analyzed sequential samples from two representative “GMP pattern” MDS patients by CyTOF (**Figures 12 and 13**).

CyTOF analysis results of BM MNCs isolated from P2 (analyzed by scRNA-seq in section 4.2.2) were consistent with the scRNA-seq analysis results. MCL1, but not BCL2, was highly expressed in the disease-driving LMPPs; and BCL2 was highly expressed in the T cell populations (**Figure 12a-c**). Additionally, a subgroup of CD4⁺ T cells expanded when P2 achieved mCR (**Figure 12d**).

P4 achieved mCR after C2 and C4 of venetoclax-based therapy and progressed to AML at C5. The Lin⁻CD34⁺ HSPCs of P4 expressed high levels of MCL1 but not BCL2 (**Figure 13a and b**). Along with a dramatic expansion of the LMPP population at C5 (PD) (**Figure 13c**), these results consistently validate our lab’s previous findings that LMPPs depend on NF-κB signaling pathways for survival in order to drive disease progression in “GMP pattern” MDS. Likewise, BCL2 was highly expressed in T cells (**Figure 13b and c**) and a CD4⁺ T cell population expanded when the patient responded to venetoclax-based therapy, indicating that the response to venetoclax-based therapy in “GMP pattern” MDS patients could be mediated by T cells instead of being the result of venetoclax-mediated direct targeting of HSCs.

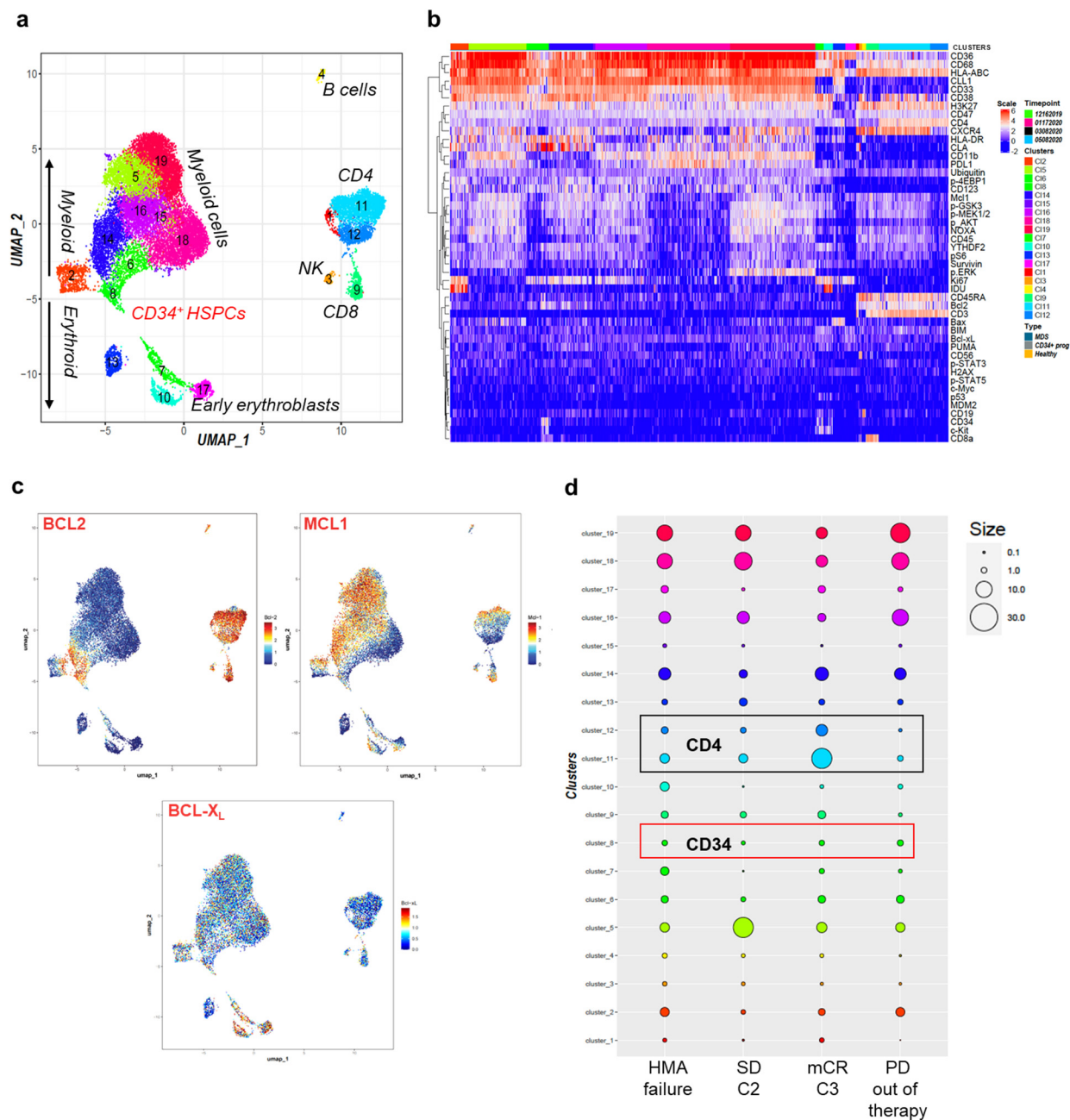


Figure 11. Cytometry by time of flight (CyTOF) analysis of BM MNCs isolated from sequential BM samples from a representative “CMP pattern” MDS patient (P3).

(a) Visualization of t-distributed stochastic neighbor embedding (viSNE) plot of MNCs cells from 4 sequential samples isolated from a “CMP pattern” MDS patient after HMA failure. **(b)** Heatmap of protein expression among the cell clusters at different time points during

venetoclax-based therapy. **(c)** viSNE plots of MNCs from the 4 sequential samples showing the expression of the BCL2 family proteins BCL2, MCL1, BCL-X_L. **(d)** Dot plots showing the cell cluster size at each therapy time point (SD, stable disease; C2, cycle 2 of venetoclax-based therapy; C3, cycle 3 of venetoclax-based therapy; mCR, marrow complete remission; PD, progressive disease)

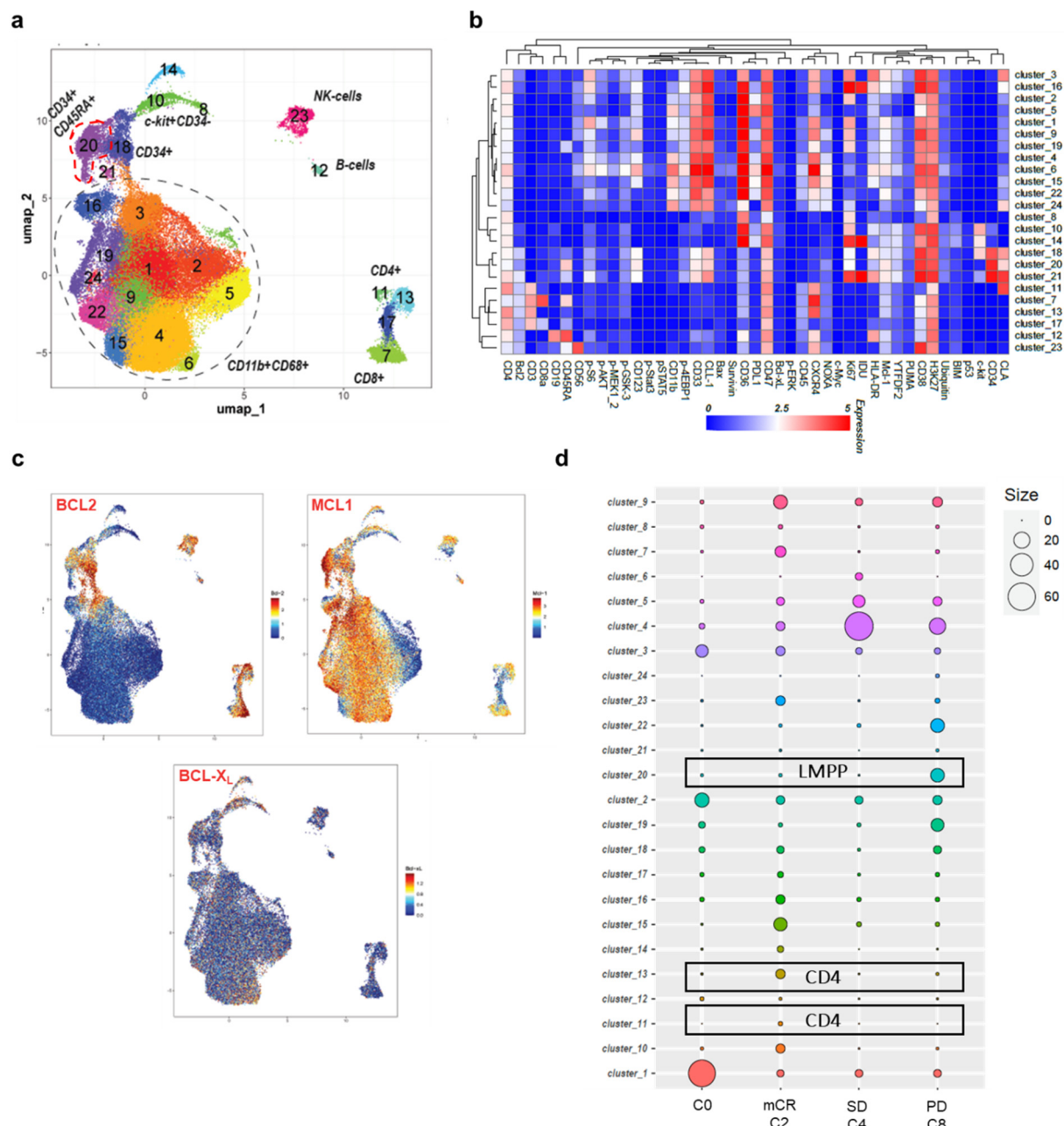


Figure 12. Cytometry by time of flight (CyTOF) analysis in BM MNCs isolated from sequential BM samples of a representative “GMP pattern” MDS patient (P2).

(a) viSNE plot of MNCs cells from 4 sequential samples isolated from a “GMP pattern” MDS patient (P2). **(b)** Heatmap of protein expression among the cell clusters at different time points during venetoclax-based-therapy. **(c)** viSNE plots of MNCs from the 4 sequential samples showing the expression of the BCL2 family proteins BCL2, MCL1, BCL-X_L. **(d)** Dot plots showing the cell cluster size at each therapy time point (mCR, marrow complete remission; C2, cycle 2 of venetoclax-based therapy; SD, stable disease; C4, cycle 4 of venetoclax-based therapy; PD, progressive disease; C8, cycle 8 of venetoclax-based therapy).

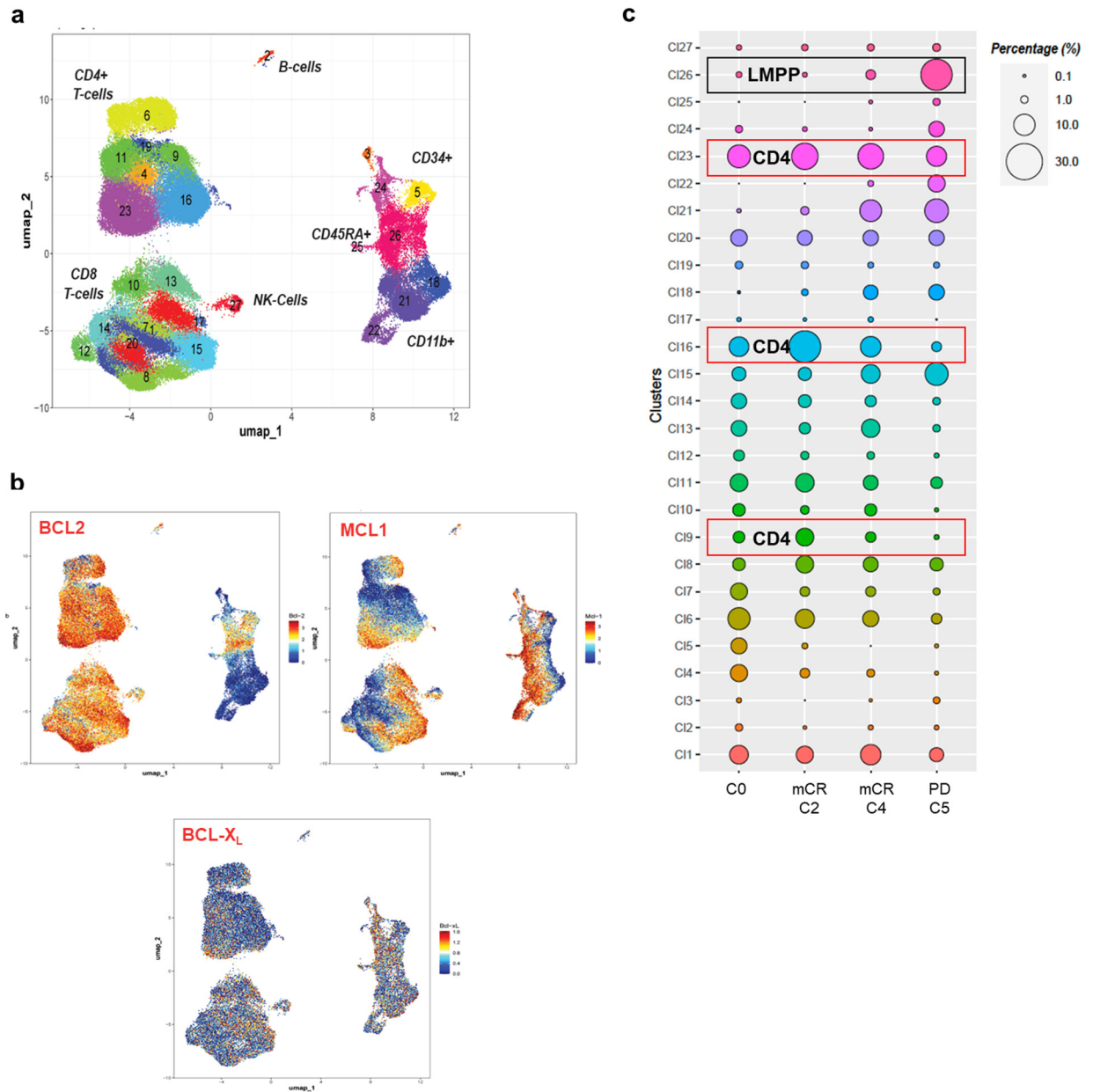


Figure 13. Cytometry by time of flight (CyTOF) analysis in BM MNCs isolated from the sequential BM samples from a representative “GMP pattern” MDS patient (P4).

(a) viSNE plot of MNCs cells from 4 sequential samples isolated from a “GMP pattern” MDS patient. **(b)** viSNE plots of MNCs from the 4 sequential samples showing the expression of the BCL2 family proteins BCL2, MCL1, and BCL-XL. **(c)** Dot plots showing the cell cluster size at each therapy time point (mCR, marrow complete remission; C2, cycle 2 of venetoclax-based

therapy; C4, cycle 4 of venetoclax-based therapy; PD, progressive disease; C5, cycle 5 of venetoclax-based therapy).

4.4. T Cell Analyses by Flow Cytometry

Preliminary results of scRNA-seq and CyTOF analyses in sequential BM samples isolated from MDS patients enrolled in venetoclax-based clinical trials revealed that a subtype of CD4⁺ T cells expanded when patients achieved mCR. Therefore, we performed T cell analysis by flow cytometry to identify the specific population that significantly changed during response to venetoclax-based therapy. We analyzed BM MNCs isolated from sequential BM samples obtained from 10 MDS patients enrolled in the clinical trials and quantified the frequencies of the NK and T cell populations at different therapy times in correlation with the type of clinical response. Specifically, we analyzed NK CD16^{hi}, NK CD16^{lo}, CD4⁺ T cells, CD8⁺ T cells, naïve T cells (T_N), stem cell memory T cells (T_{SCM}), terminal effector T cells (T_E), effector memory T cells (T_{EM}), central memory T cells (T_{CM}), regulatory T cells (T_{reg}), and CD45RO⁺CD45RA⁺ T cells based on their surface and intracellular markers (**Table 2**). We did not observe any significant change in the frequencies of total CD4⁺ T cells, CD8⁺ T cells, and NK cells in the BM MNCs over the course of the disease (**Figure 14**). However, our further analysis of the specific sub-populations inside the CD4⁺, CD8⁺, and NK compartments revealed that the CD4⁺ T_{SCM} significantly expanded in the BM of patients who achieved mCR (**Figure 15**). Similar data were obtained when we analyzed the CD4⁺ T_{SCM} frequency inside the CD4⁺ T cell compartment (**Figure 16**), as well as when we performed paired analysis of these cells in sequential samples (**Figure 17**). Interestingly, our paired analyses also showed that the CD4⁺ naïve T cell (T_N) population increased when patients had mCR (**Figure 17**). These findings are consistent with the results obtained by our scRNA-seq and CyTOF analyses showing that CD4⁺ T cell populations with a naïve and/or early-activated antigen-experienced phenotype, such as T_N and T_{SCM}, expanded in the BM of patients who achieved mCR.

Consistent with our previous data, we did not observe any significant change in the CD8⁺ T cell subpopulations within either BM MNCs (**Figure 18**) or total CD8⁺ T cells (**Figure 19**) during venetoclax-based treatment.

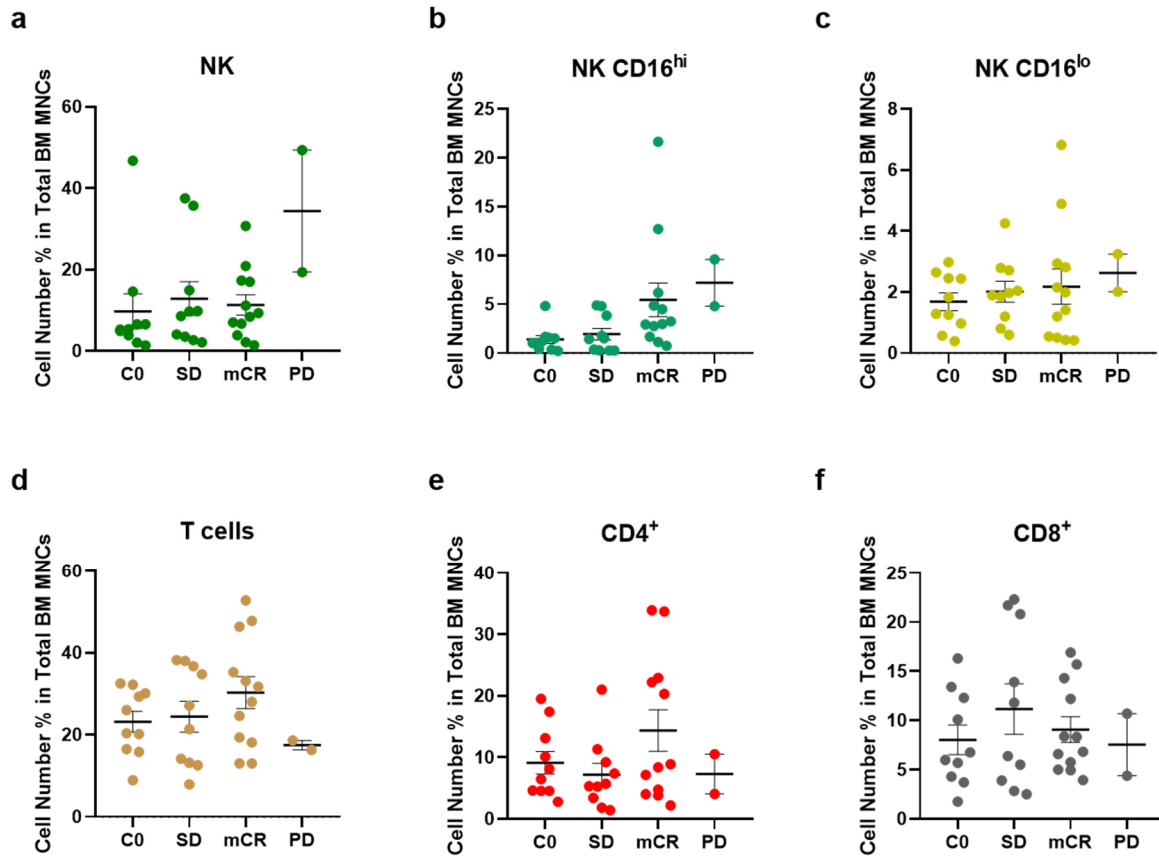


Figure 14. T and NK cell quantification by flow cytometry.

Frequencies of **(a)** NK – natural killer cells, **(b)** NK cells with high surface expression of CD16, **(c)** NK cells with low surface expression of CD16, **(d)** T cells, **(e)** CD4⁺ T cells, and **(f)** CD8⁺ T cells in total BM MNCs from MDS patients (n=10). Samples were collected when patients were enrolled into the clinical trials (C0) and during venetoclax-based therapy, at the times of stable disease (SD), marrow complete remission (mCR), and progressive disease (PD). Data are presented as means ± SEMs.

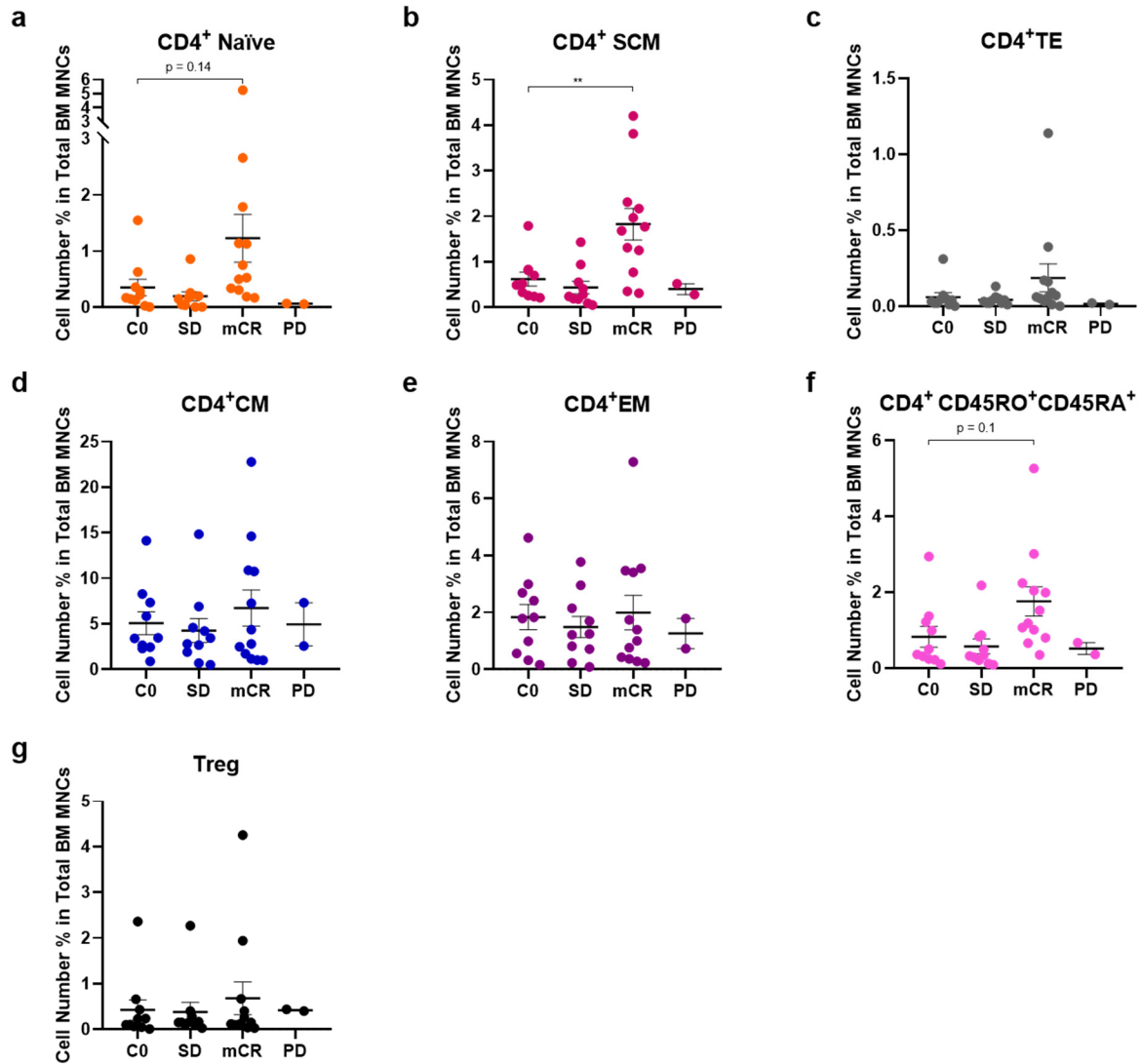


Figure 15. CD4⁺ T cell quantification in BM MNCs by flow cytometry.

Frequencies of **(a)** CD4⁺ naïve T cells, **(b)** CD4⁺ stem cell memory T cell (SCM), **(c)** CD4⁺ terminal effector cells (TE), **(d)** CD4⁺ central memory T cells (CM), **(e)** CD4⁺ effector memory T cells (EM), **(f)** CD4⁺CD45RO⁺CD45RA⁺ T cells, and **(g)** regulatory T cells (T_{reg}) from MDS patients (n=10) in total BM MNCs. Samples were collected when patients were enrolled into the clinical trials (C0) and during venetoclax-based therapy, at the times of stable disease (SD), marrow complete remission (mCR), and progressive disease (PD). Data are presented as means ± SEMs.

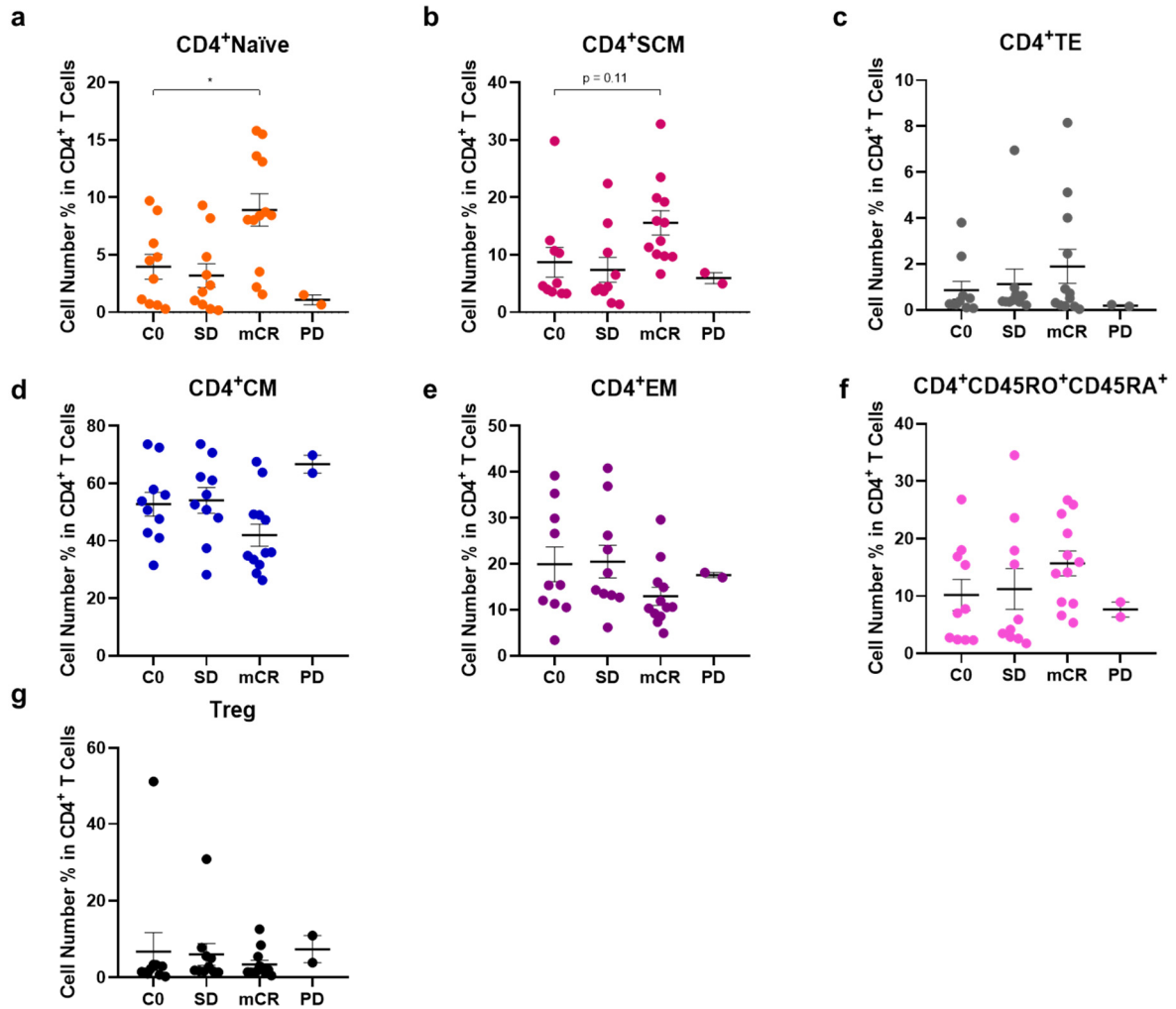


Figure 16. CD4⁺ T cell quantification in the CD4⁺ T cell compartment by flow cytometry.

Frequencies of **(a)** CD4⁺ naïve T cells, **(b)** CD4⁺ stem cell memory T cell (SCM), **(c)** CD4⁺ terminal effector T cells (TE), **(d)** CD4⁺ central memory T cells (CM), **(e)** CD4⁺ effector memory T cells (EM), **(f)** CD4⁺CD45RO⁺CD45RA⁺ T cells, and **(g)** regulatory T cells (T_{reg}) in total CD4⁺T cells from MDS patients (n=10). Samples were collected when patients were enrolled into the clinical trials (C0) and during venetoclax-based therapy, at the times of stable disease (SD), marrow complete remission (mCR), and progressive disease (PD). Data are presented as means ± SEMs.

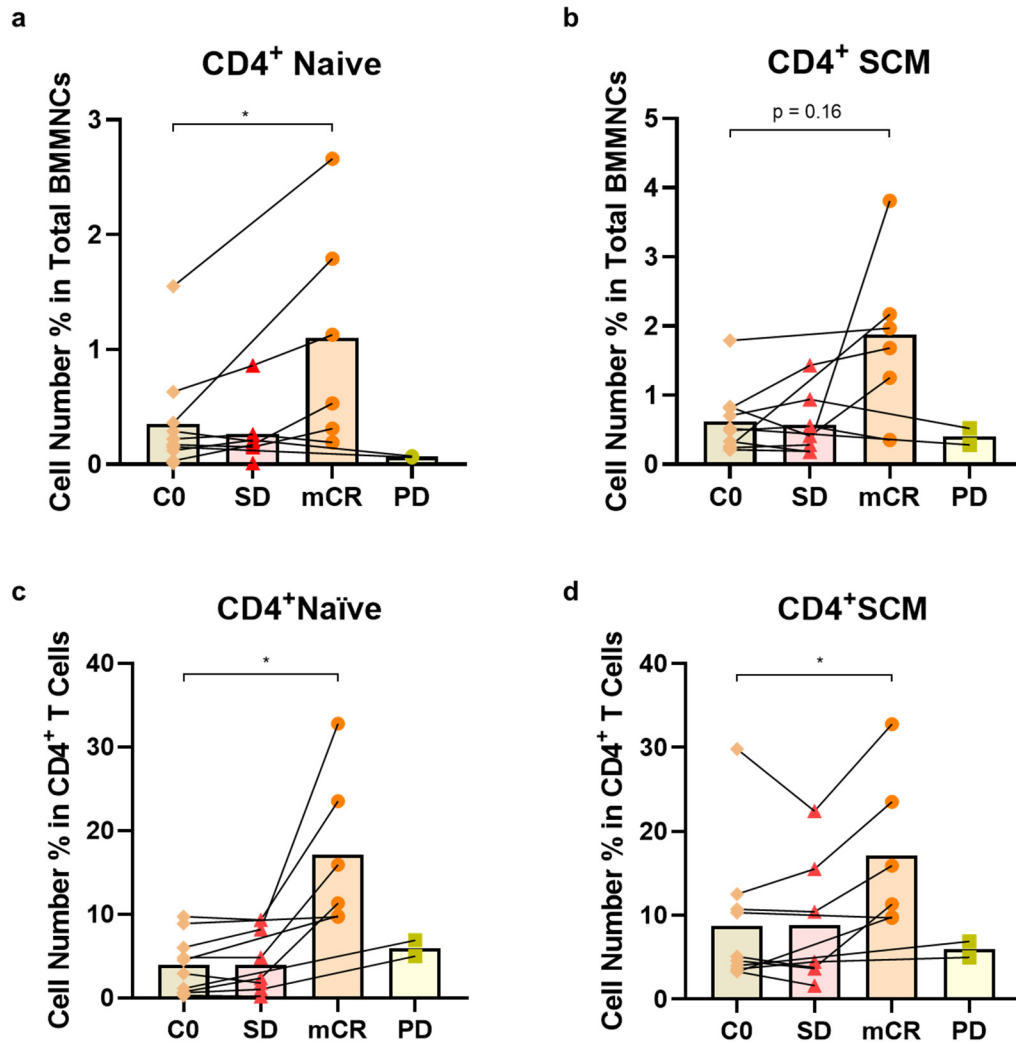


Figure 17. CD4⁺ T cell quantification in sequential patient samples by flow cytometry

Frequencies of **(a)** CD4⁺ naïve T cells, **(b)** CD4⁺ stem cell memory T cell (SCM). Cell number % in total T CD4⁺ cells of **(c)** CD4⁺ naïve T cells, **(d)** CD4⁺ stem cell memory T cell (SCM) in total BM MNCs from MDS patients (n=10). Samples were collected when patients were enrolled into the clinical trials (C0) and during venetoclax-based therapy, at the times of stable disease (SD), marrow complete remission (mCR), and progressive disease (PD). Only paired samples were analyzed, and data are presented as means \pm SEMs.

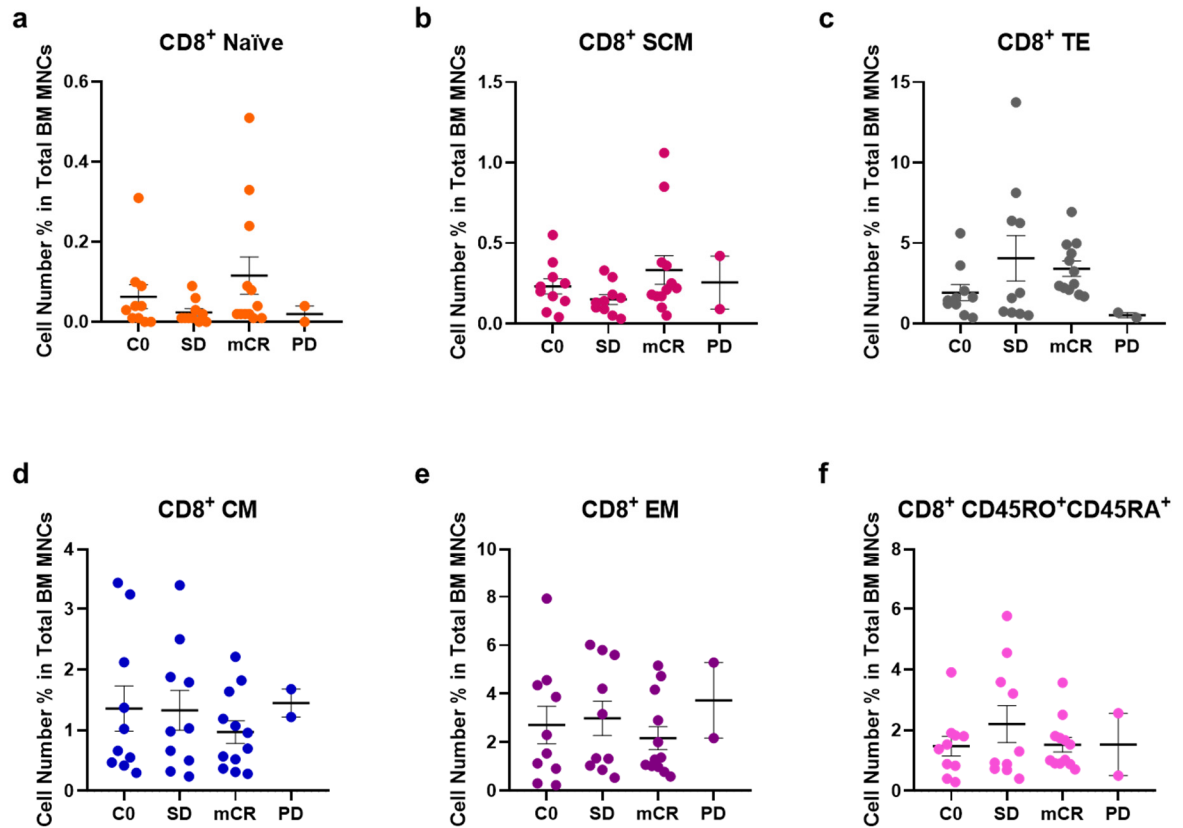


Figure 18. CD8⁺ T cell quantification in BM MNCs by flow cytometry.

Frequencies of **(a)** CD8⁺ naïve T cells, **(b)** CD8⁺ stem cell memory T cell (SCM), **(c)** CD8⁺ terminal effector T cells (TE), **(d)** CD8⁺ central memory T cells (CM), **(e)** CD8⁺ effector memory T cells (EM), **(f)** CD8⁺CD45RO⁺CD45RA⁺ T cells in total BM MNCs from MDS patients (n=10). Samples were collected when patients were enrolled in the clinical trials (C0) and during venetoclax-based therapy, at the times of stable disease (SD), marrow complete remission (mCR), and progressive disease (PD). Data are presented as means \pm SEMs.

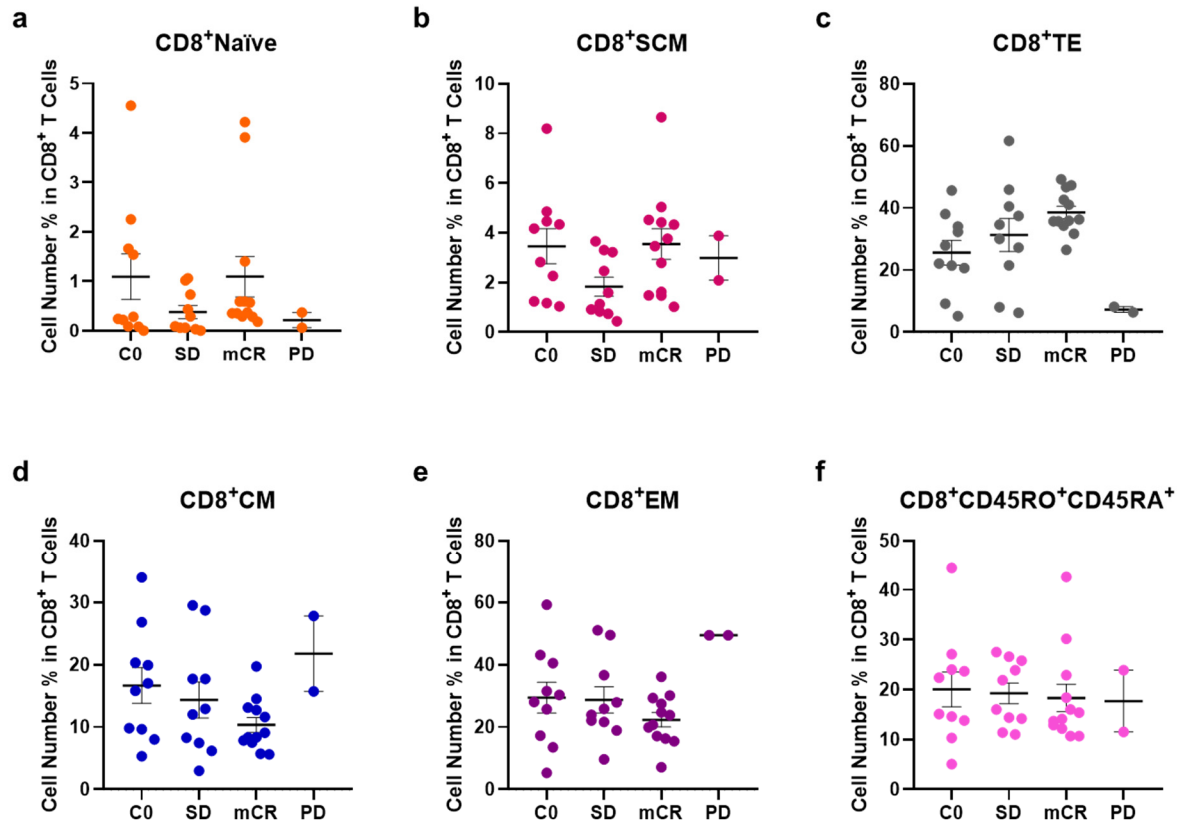


Figure 19. CD8⁺ T cell quantification in the CD8⁺ compartment by flow cytometry.

Frequencies of **(a)** CD8⁺ naïve T cells, **(b)** CD8⁺ stem cell memory T cell (SCM), **(c)** CD8⁺ terminal effector T cells (TE), **(d)** CD8⁺ central memory T cells (CM), **(e)** CD8⁺ effector memory T cells (EM), **(f)** CD8⁺CD45RO⁺CD45RA⁺ T cells in CD8⁺ compartment from MDS patients (n=10). Samples were collected when they were enrolled in the clinical trials (C0) and during venetoclax-based therapy, at the times of stable disease (SD), marrow complete remission (mCR), and progressive disease (PD). Data are presented as means ± SEMs.

4.5 Assessing the Feasibility of Targeting MCL1 in Venetoclax-Resistant MDS

4.5.1 The combination of venetoclax and AMG-176 can synergistically eradicate MDS-L cells *in vitro*.

Results from our scRNA-seq and CyTOF analyses suggested that MCL1, but not BCL2, is highly expressed in both HSPCs and blasts from “GMP pattern” MDS. We, therefore, hypothesized that MCL1 inhibition could effectively target MDS stem cells in BCL2-negative, thus venetoclax-resistant MDS. To test the hypothesis, we performed pre-clinical studies using the MCL1 inhibitor AMG-176. First, we treated the MDS-L cell line, the only available cell line in MDS research, with venetoclax and AMG-176 as single agents or in combination. The MDS-L line was established from a patient with MDS at the time of disease progression [73] and expresses both BCL2 and MCL1 (**Figure 20a**). We observed that MDS-L cells were highly resistant to 48-hour single-agent treatments with either venetoclax ($IC_{50} \approx 1 \mu M$) or AMG-176 ($IC_{50} > 10 \mu M$) (**Figure 20b-e**). However, the combination of venetoclax (200 nM) and AMG-176 (200 nM, 500 nM) could significantly induce apoptosis in MDS-L cells, as shown by Annexin V/DAPI analysis by flow cytometry (**Figure 21a, b**). Taken together, these results suggested that BCL2 inhibition by venetoclax and MCL1 inhibition by AMG-176 could synergistically eradicate venetoclax-resistant MDS-L cells.

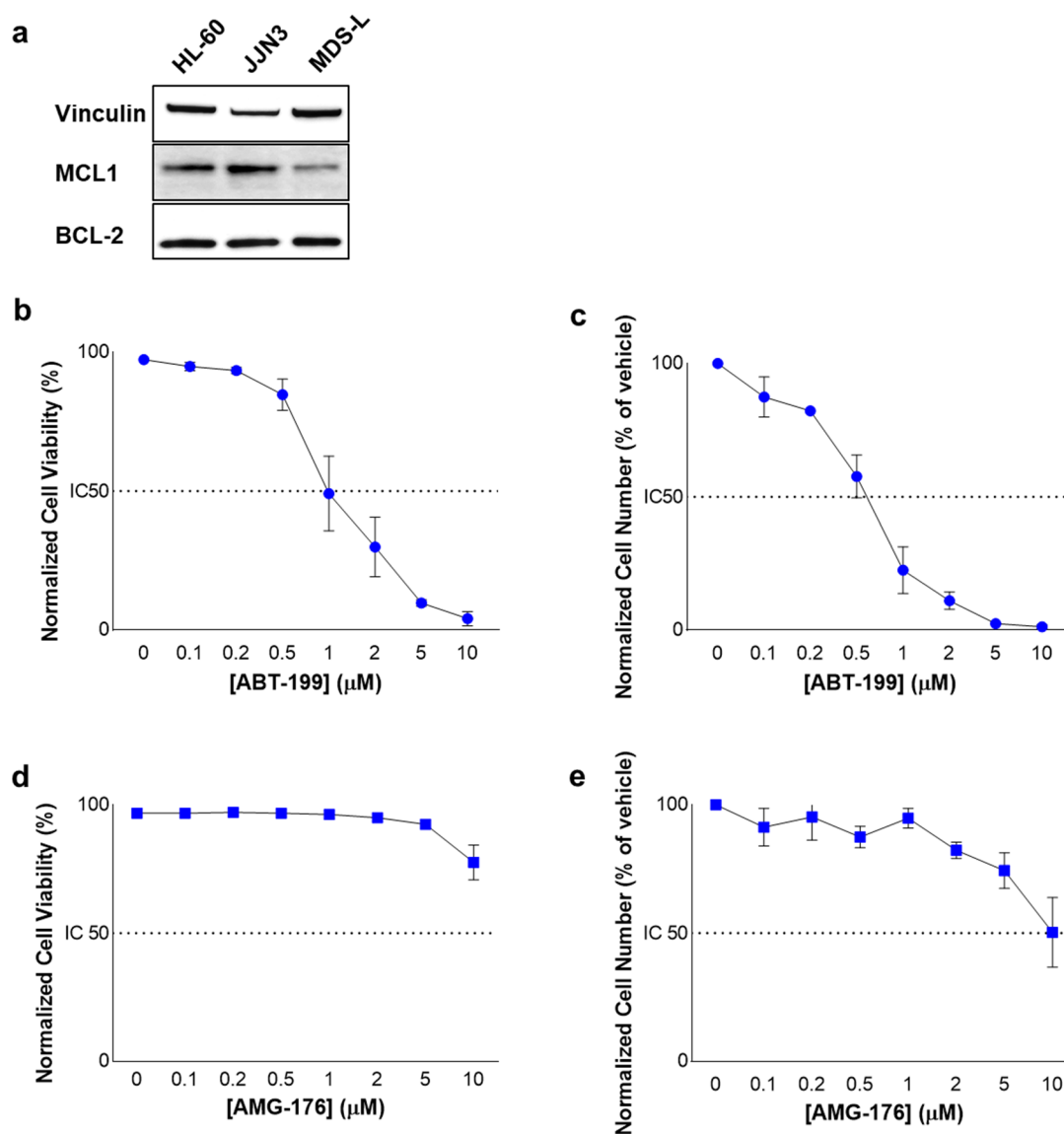


Figure 20. Effect of single-agent treatments with venetoclax (ABT-199) and AMG-176 on MDS-L cells.

(a) Western blot showing MCL1 and BCL2 expression in MDS-L cells. Vinculin was used as loading control. HL-60 and JJN3 cells were used as positive controls. **(b, c)** Effect of ABT-199 treatment on MDS-L **(b)** cell number and **(c)** cell viability. MDS-L cells were treated *in vitro* with vehicle (DMSO) or increasing concentrations of ABT-199 for the indicated time points. **(d, e)** The effect of AMG-176 treatment on MDS-L **(d)** cell number and **(e)** cell viability. MDS-L cells were treated *in vitro* with vehicle (DMSO) or increasing concentrations of AMG-176 for 48

hours. Data were normalized to the vehicle-treated controls and are presented as means \pm SEMs.

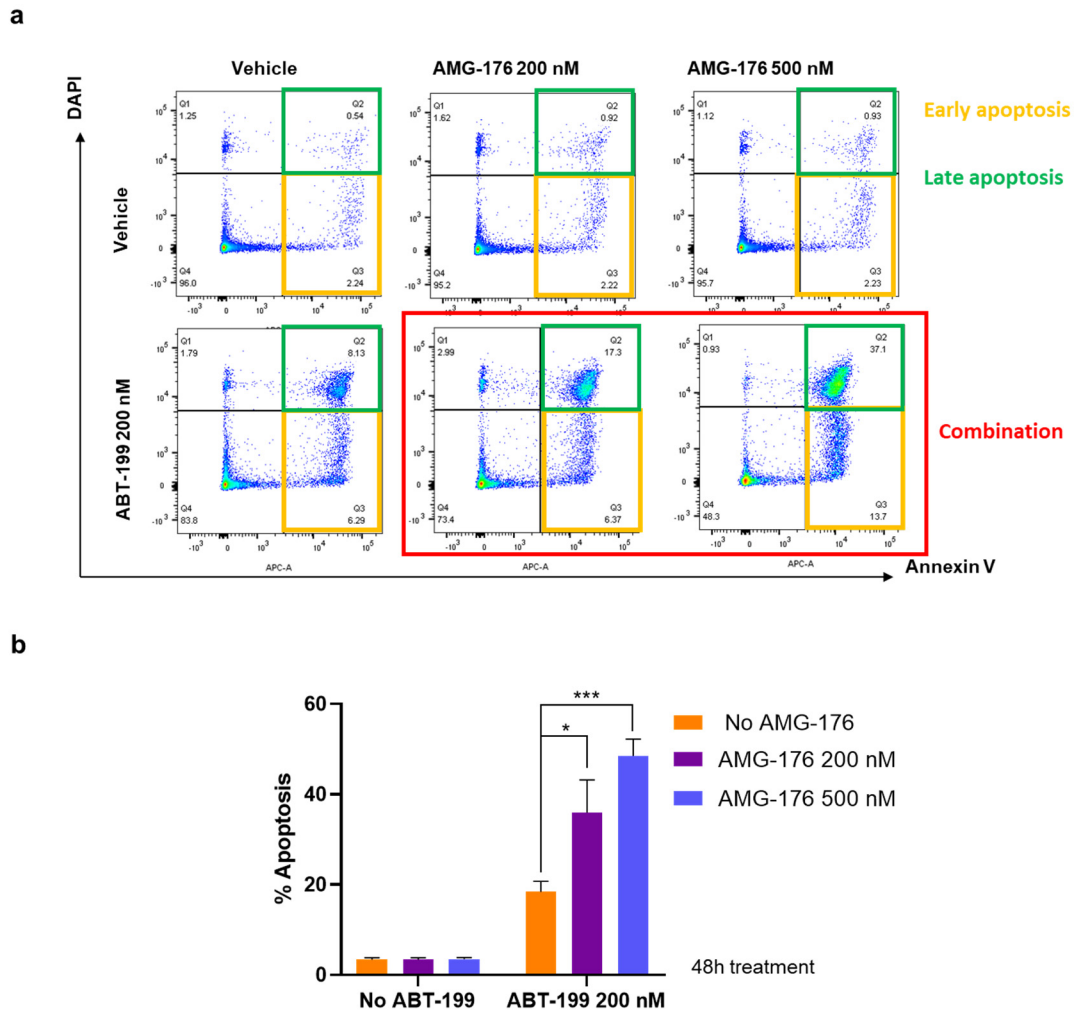


Figure 21. Apoptosis analysis and quantification in MDS-L cells after treatment with venetoclax (ABT-199) and AMG-176, as single agents and in combination.

(a) Representative flow cytometry plots of apoptosis analysis by Annexin V/DAPI staining in MDS-L cells treated with vehicle (DMSO) and 200 nM of ABT-199 alone or in combination with 200 or 500 nM of AMG-176 *in vitro* for 48 hours. **(b)** Frequency of MDS-L cells that underwent apoptosis after being treated with 200 nM of ABT-199 and 200 nM or 500 nM of ABT-176 as single agents or in combination for 48 hours *in vitro*. Data are presented as means \pm SEMs.

4.5.2 The combination of venetoclax and AMG-176 can synergistically suppress MDS stem cell survival *in vitro*.

Next, we sought to evaluate whether AMG-176 as a single agent or in combination with venetoclax could eradicate venetoclax-resistant MDS stem cells. We isolated Lin⁻CD34⁺ HSPCs from MDS patients, co-cultured them with human mesenchymal stromal cells (MSCs) isolated from healthy donors and treated the co-cultures with venetoclax and AMG-176 as single agents or in combinations at a safe dose that spared normal HSPCs for 48 hours (**Figure 22a, b**). Harvested cells were quantified by flow cytometry. We observed that in “CMP pattern” MDS the Lin⁻CD34⁺CD38⁻ HSCs were sensitive to venetoclax as a single agent (**Figure 22c**), which supported our previous finding that BCL2 inhibition by venetoclax could selectively eradicate the disease-driving stem cells in “CMP pattern” MDS. In addition, single-agent treatment with AMG-176 at 50 nM also significantly decreased the number of disease-driving stem cells, the effect of which was further enhanced by combining AMG-176 with venetoclax (**Figure 22d**). In contrast, the Lin⁻CD34⁺CD38⁻ HSCs from “GMP pattern” MDS patients were not sensitive to the single-agent treatments with venetoclax or AMG-176 but responded to the combination treatment. Altogether, these results demonstrate the therapeutic potential of MCL1 inhibition by AMG-176 in combination with venetoclax to effectively eradicate venetoclax-resistant MDS blasts and disease-driving HSCs *in vitro*.

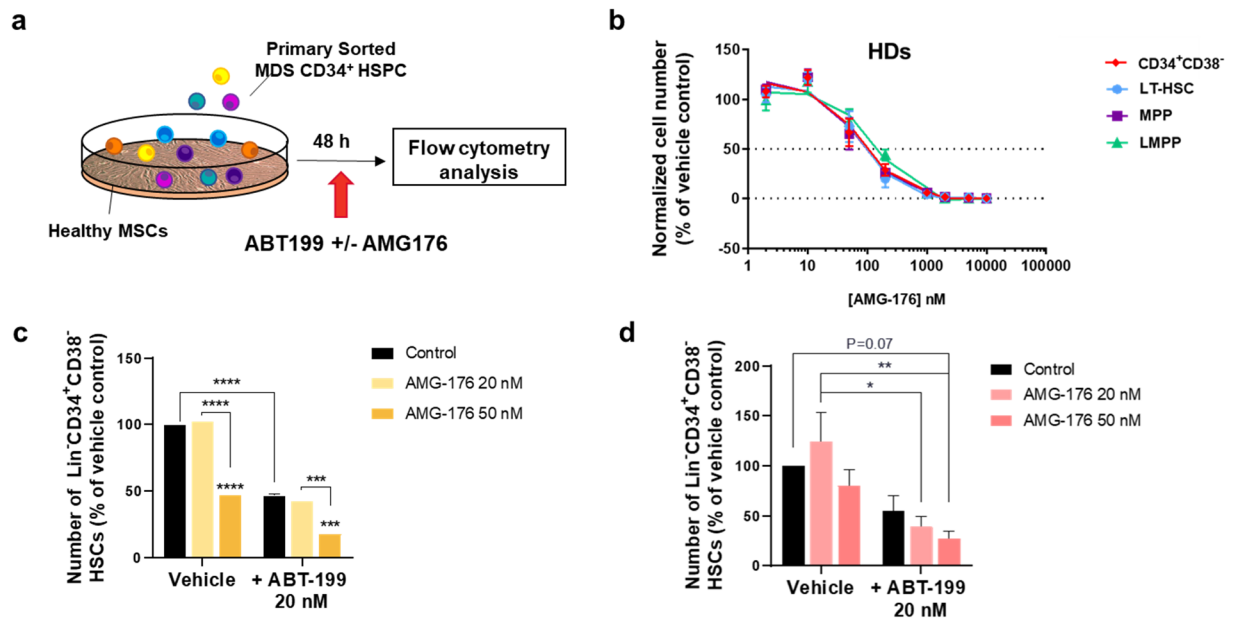


Figure 22. Effect of single-agent and combination treatments with venetoclax (ABT-199) and AMG-176 in primary MDS HSCs.

(a) Diagram representing the co-culture system of MDS CD34⁺ HSPCs with healthy human MSCs. Cells were treated with venetoclax (ABT-199) and AMG-176 as single agents or in combination for 48 hours, followed by flow cytometry analysis. **(b)** Dose-response curves showing the numbers of live CD34⁺CD38⁻ HSCs, long-term hematopoietic stem cells (LT-HSCs), multipotent progenitors (MPPs), and lymphoid-primed multipotent progenitors (LMPPs) from the BM of healthy donors after 48 h of treatment with increasing doses of AMG-176. Data were normalized to the vehicle-treated controls and are presented as means \pm SEMs (n=3 samples). **(c, d)** Numbers of live CD34⁺CD38⁻ cells from samples of “CMP pattern” MDS (n=2) **(c)** or “GMP pattern” MDS (n=9) **(d)** at disease progression after treatment with vehicle or AMG-176 at the indicated doses in the presence or absence of 20 nM venetoclax (ABT-199). Data were normalized to the vehicle-treated controls and are presented as means \pm SEMs.

4.5.3 The combination of venetoclax and AMG-176 can significantly decrease BM chimerism in a “GMP pattern” MDS patient-derived xenograft (PDX).

To investigate whether AMG-176 as a single agent or in combination with venetoclax could effectively reduce venetoclax-resistant tumor burden *in vivo*, we established a PDX model of venetoclax-resistant MDS by transplanting T cell-depleted BM MNCs isolated from a “GMP pattern” MDS patient into NSG-SGM3 mice (**Figure 23a**). Based on our previous findings, cells from this patient were predicted to be resistant to treatment with venetoclax. Indeed, the blasts from this “GMP pattern” MDS PDX model were resistant to venetoclax and AMG-176 as single agents following two weeks of treatment, but they were sensitive to the combination of both agents, as indicated by the significant decrease in the chimerism of human CD45⁺ cells in the BM (**Figure 23b**). These results suggest that the combination of venetoclax and AMG-176 can overcome venetoclax resistance *in vivo*.

We had also transplanted T cell-depleted BM MNCs isolated from a venetoclax-resistant “CMP pattern” MDS patient into NSG-SGM3 mice. Unfortunately, due to the non-engraftment of these cells into the mice after 12 weeks, we could not start the treatments. This was not due to our technical deficiency, but it was the result of the intrinsic inability of MDS cells to reconstitute hematopoiesis in recipient mice.

Of note, our studies also highlight that the PDX models possibly fail to faithfully recapitulate and mimic complex diseases, such as MDS, in which the adaptive immune response plays a fundamental role in achieving disease remission after therapy.

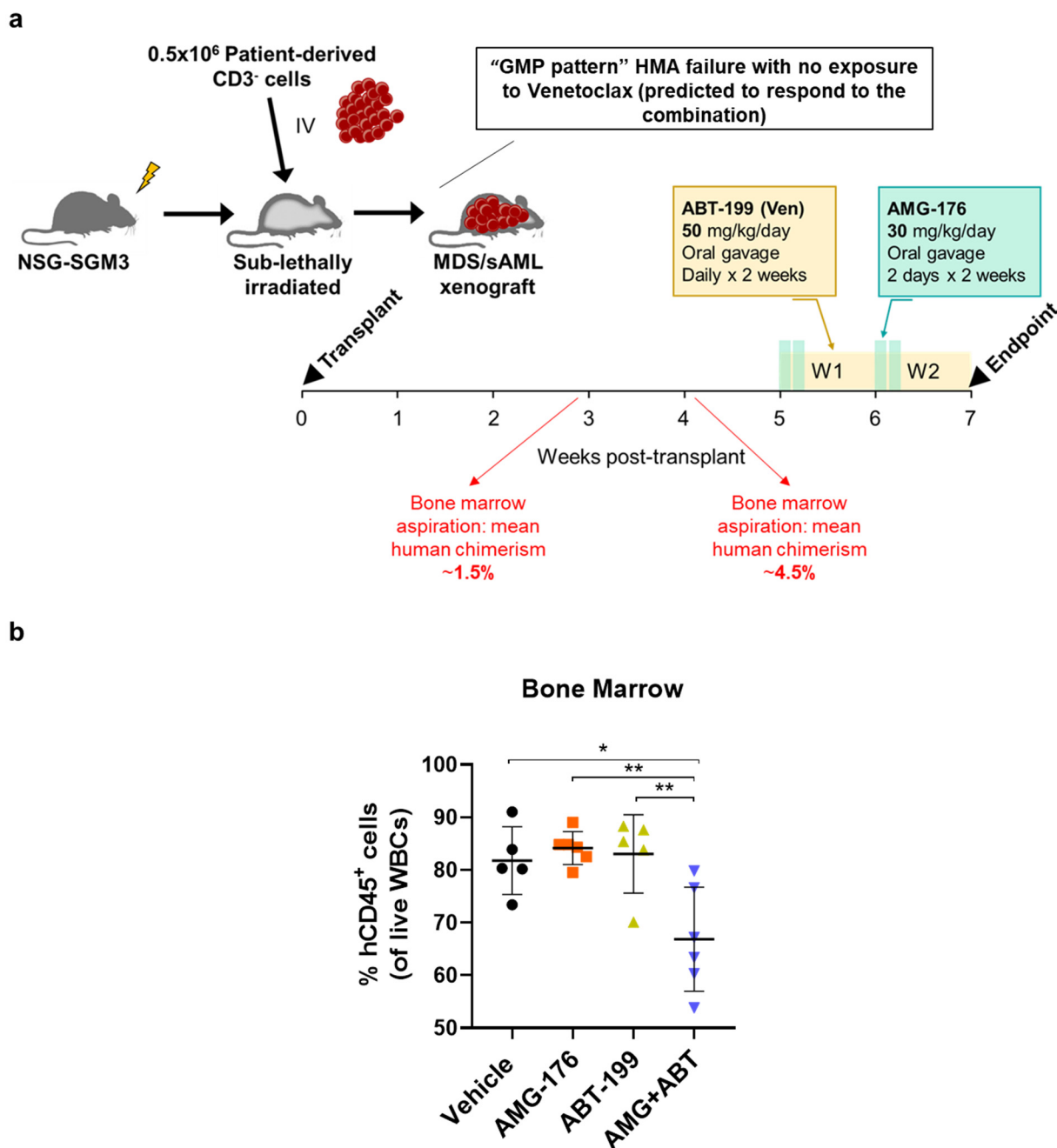


Figure 23. Effect of single-agent and combination treatments with venetoclax (ABT-199) and AMG-176 on a representative “GMP pattern” MDS patient-derived xenograft model (PDX).

(a) Schematic image of the PDX experiment. NSG-SGM3 mice (n=22) were sub-lethally irradiated and injected with 0.5x10⁶ patient-derived T cell-depleted (CD3⁺) MNCs. Mice were

treated with 50 mg/kg/day of ABT-199 daily by oral gavage for two weeks and/or with 30 mg/kg/day AMG-176 on the first two days of the week for two weeks. At the endpoint, chimerism was assessed in the BM by flow cytometry. **(b)** Frequencies of human CD45⁺ cells in BM cells from xenografts developed from a representative “GMP pattern” MDS sample after treatment with vehicle, AMG-176, ABT-199, or the combination of both agents (AMG+ABT). Bars represent the means \pm SEMs.

CHAPTER 5: DISCUSSION

Previous studies that involved high-throughput next-generation sequencing techniques demonstrated that MDS are maintained and propagated by HSCs with cumulative somatic mutations [74]. Our lab revealed that two different immunophenotypically distinct hierarchical cellular organizations of MDS HSPCs contribute to therapy resistance and disease progression by the upregulation of specific survival pathways. As explained in the introduction section of this Thesis, MDS patients can be stratified into two subtypes based on their immunophenotypic hierarchies: “CMP pattern” and “GMP pattern” MDS. “CMP pattern” MDS were characterized by having an increased frequency of the CMPs among MyHPCs and an expansion of the LT-HSCs driven by BCL2-mediated anti-apoptotic mechanisms following HMA failure. “GMP pattern” MDS were defined by having an increased frequency of the GMPs among the MyHPCs and an expansion of the LMPPs driven by NF- κ B-mediated survival pathways following HMA failure. Our preclinical results demonstrated that the inhibition of the survival pathways driving each MDS subgroup’s progressive disease could selectively eradicate the respective MDS stem cells and decrease tumor burden in PDX models.

In our study, we employed the BCL2 inhibitor venetoclax (ABT-199). Clinical trials of venetoclax-based therapy for MDS patients who have failed previous therapies are ongoing at MD Anderson Cancer Center, allowing us to validate our preclinical findings through correlative studies. Indeed, the preliminary data presented in this study support the hypothesis that targeting BCL2 with venetoclax can elicit a durable response in “CMP pattern” MDS. As more eligible MDS patients are recruited, we expect to update the results with a larger sample cohort to validate this conclusion.

The development of novel therapeutics should include the identification of potential mechanisms of response and resistance in order to appropriately design clinical studies and potentially include precise and effective combination therapies. Therefore, we sought to identify

biomarkers of venetoclax response and resistance in MDS by employing scRNA-seq and CyTOF to analyze sequential BM samples from MDS patients enrolled in prospective clinical trials of venetoclax for the treatment of HMA-resistant MDS. Our scRNA-seq and IHC data showed that BCL2 was not expressed in neither the HSPCs nor the blasts from BM of “CMP pattern” MDS patients with a *TP53* mutation or “GMP pattern” MDS patients. However, T cells from both types of MDS subgroups expressed BCL2 and underwent significant population changes, indicating that the initial response to venetoclax therapy was not due to the direct targeting of either disease-driving HSPCs or blast populations but it was the results of the adaptive T cell response.

Throughout various clinical studies, it has been demonstrated that *TP53* mutations in cancer patients were correlated with poor clinical outcomes and poor prognosis with venetoclax-based therapy [75]. Furthermore, loss of function of TP53 can confer cancer cell resistance to BCL2 inhibition by perturbing gene expression of pro-apoptotic BCL2 family proteins and decreasing the level of BCL2 expression [75]. Together with the IHC BCL2 quantification in BM biopsies from *TP53*-mutated MDS, our study suggests that *TP53* mutations and BCL2 expression are mutually exclusive. These data also suggest that *TP53*-mutant MDS patients should be treated with specific inhibitors of mutant TP53, such as APR-246 [76].

In addition, our data show that *MCL1* was expressed in the majority of blasts and HSPCs of the *TP53*-mutated “CMP pattern” MDS patient and was highly expressed in LMPPs of all “GMP pattern” MDS patients. Because *MCL1* is one of the downstream transcriptional targets of NF- κ B [64], these results are consistent with our previous study showing that LMPPs of “GMP pattern” MDS patients rely on the upregulation of the NF- κ B survival pathway to maintain and propagate the disease. These results also suggest that *MCL1* expression may be

one of the mechanisms that account for venetoclax resistance in MDS, leading to our hypothesis that MCL1 inhibition can effectively target leukemogenic stem cells in venetoclax-resistant MDS. Our preclinical results demonstrate that MCL1 inhibition by the small-molecule BH3 mimetic AMG-176 in combination with venetoclax can eradicate MDS blasts and stem cells *in vitro* and reduce venetoclax-resistant tumor burden *in vivo*. Altogether, our study substantiates the feasibility of targeting MCL1 by AMG-176 to overcome venetoclax resistance in MDS. Recently, a phase I/II clinical trial to evaluate the safety and activity of AMG-176-based therapy in MDS patients who have failed prior therapy and developed progressive disease has been initiated at MD Anderson Cancer Center (MDACC 2021-0276). Future correlative studies using samples from patient enrolled in this clinical trial will assess the efficacy of AMG-176-based therapy in targeting MDS HSCs.

Apart from the response or resistance of MDS blasts and HSPCs to venetoclax therapy, we observed changes in the frequencies of the CD4⁺ T cell populations during venetoclax-based treatment, which suggests a role of the adaptive immune system in venetoclax response. ScRNA-seq analysis revealed that a subset of naïve and/or early-activated antigen-experienced CD4⁺T cells with expression of *CCR7*, *CD28*, and *CD27* was enriched only when MDS patients achieved mCR. Based on the hierarchical model of T cell differentiation, naïve T cells (T_N) undergo rapid proliferation and differentiation upon antigen recognition. They can generate effector T cells (T_E) for immediate immune response to eradicate pathogens or differentiate into long-lived memory T cells that respond to recurrent antigens and maintain long-term immune surveillance [77]. The memory T cell subsets include effector memory T cells (T_{EM}), central memory T cells (T_{CM}), and stem cell memory T cells (T_{SCM}) [60]. Our T cell analysis results showed a significant increase in populations of CD4⁺T_N and T_{SCM} in the bone marrow of MDS patients at the time when they responded to venetoclax-based therapy, suggesting enhanced T_N activation during the response. The rise of T_{SCM}, therefore, might be a

consequence of rapid T_N differentiation. Our results suggest that, when MDS patients respond to venetoclax-based therapy, their naïve T cells undergo rapid proliferation and differentiation, preferentially to T_{SCM} , which may be one potential mechanism that induces favorable outcomes to venetoclax treatment. However, the factors that contribute to T_N activation and whether this is induced directly by venetoclax remain unknown. Previous studies demonstrated that T_N could be stimulated by antigen presentation and cytokine secretion of dendritic cells or by pro-inflammatory cytokines in an antigen-independent manner [78]. Reduced effectiveness of antigen presentation resulting from an immunosuppressive tumor microenvironment (TME) can lead to insufficient T cell activation and exertion of an anti-tumor response [79]. Thus, it is possible that the increased proliferation of T_N was due to enhanced and prolonged antigen presentation induced by venetoclax treatment.

T_{SCM} is a rare subset of long-lasting memory T cells that possess the ability of self-renewal and exhibit effector functions, including TNF- α , interferon-gamma (IFN- γ), and interleukin-2 (IL-2) secretion [59]. They were first described by Gattinoni *et al.* in 2011 as a subset of memory T cells that maintained stem cell-like properties, had increased proliferation capacity and efficiency of reconstitution, and displayed enhanced anti-tumor activity in a humanized mouse model compared with naïve and other memory T cell subsets [80]. Later, studies have shown that T_{SCM} plays an essential role in directing anti-tumor response and maintaining long-term immune surveillance in various types of cancers [59]. These properties make T_{SCM} a great candidate for adoptive immunotherapy [81]. Thus, in our case, the increase in the T_{SCM} population upon response to venetoclax-based therapy might indicate an enhanced anti-tumor activity against leukemic cells mediated by T cells. However, the mechanisms by which the increased T_{SCM} in BM potentially contribute to leukemic cell eliminations need to be further investigated. Since T_{SCM} possesses a superior ability to self-renew and differentiate into downstream memory and effector cells to exert rapid immune response [80], the elevation of

T_{SCM} in venetoclax responders might consequently generate a more significant number of differentiated and activated memory and effector cells. Indeed, our data suggested that when MDS patients achieved mCR, they had an increase in transition from naïve/stem cell memory T cells to effector/central memory T cells. Therefore, upon the recurrent stimulation of a potential leukemic cell antigen, the effectiveness and efficiency of memory T cell activation in venetoclax responders may be more profound than in the non-responders. To understand whether the memory T cell subsets are clonal and can recognize antigens that are specific for leukemic cells, single-cell T cell receptor sequencing (scTCR-seq) can be performed to evaluate the specificity of T cell receptor repertoires [82].

In addition, the reasons why non-responders failed to elevate T_{SCM} population are unknown. One possible explanation is T cell exhaustion, one of the T cell dysfunctions characterized by decreased cytokine secretion and poor effector function [83]. Thus, it would be interesting to evaluate the T cell profile by scRNA-sequencing for the expression of T cell exhaustion markers [84] and investigate the polyfunctionality of T cells in venetoclax responders and non-responders, which can be assessed by performing single-cell cytokine profiling [85].

In conclusion, our T cell analysis data suggest that venetoclax response is associated with the expansion of CD4⁺T_N and T_{SCM}. Therefore, future studies should be directed toward understanding the dynamics of T cell differentiation and activation when interacting with the TME and the polyfunctionality of T cells in MDS patients who respond or are refractory to venetoclax-based therapy.

REFERENCES

1. Zhou, T., P. Hasty, C.A. Walter, A.J. Bishop, L.M. Scott, and V.I. Rebel, *Myelodysplastic syndrome: an inability to appropriately respond to damaged DNA?* Exp Hematol, 2013. **41**(8): p. 665-74.
2. Webb, D.K.H., *Myelodysplastic Syndromes*, in *Pediatric Hematology: Third Edition*. 2007. p. 405-422.
3. Zeidan, A.M., R.M. Shallis, R. Wang, A. Davidoff, and X. Ma, *Epidemiology of myelodysplastic syndromes: Why characterizing the beast is a prerequisite to taming it*. Blood Rev, 2019. **34**: p. 1-15.
4. Doulatov, S., F. Notta, E. Laurenti, and J.E. Dick, *Hematopoiesis: A human perspective*, in *Cell Stem Cell*. 2012, Elsevier Inc. p. 120-136.
5. Akashi, K., D. Traver, T. Miyamoto, and I.L. Weissman, *A clonogenic common myeloid progenitor that gives rise to all myeloid lineages*. Nature, 2000. **404**(6774): p. 193-7.
6. Reya, T., S.J. Morrison, M.F. Clarke, and I.L. Weissman, *Stem cells, cancer, and cancer stem cells*. Nature, 2001. **414**(6859): p. 105-11.
7. Zhang, Y., S. Gao, J. Xia, and F. Liu, *Hematopoietic Hierarchy – An Updated Roadmap*, in *Trends in Cell Biology*. 2018, Elsevier Ltd. p. 976-986.
8. Pellin, D., M. Loperfido, C. Baricordi, S.L. Wolock, A. Montepeloso, O.K. Weinberg, A. Biffi, A.M. Klein, and L. Biasco, *A comprehensive single cell transcriptional landscape of human hematopoietic progenitors*. Nat Commun, 2019. **10**(1): p. 2395.
9. Doulatov, S., F. Notta, E. Laurenti, and J.E. Dick, *Hematopoiesis: a human perspective*. Cell Stem Cell, 2012. **10**(2): p. 120-36.
10. Colla, S., D.S. Ong, Y. Ogoti, M. Marchesini, N.A. Mistry, K. Clise-Dwyer, S.A. Ang, P. Storti, A. Viale, N. Giuliani, K. Ruisaard, I. Ganan Gomez, C.A. Bristow, M. Estecio, D.C. Weksberg, Y.W. Ho, B. Hu, G. Genovese, P. Pettazzoni, A.S. Multani, S. Jiang, S. Hua, M.C. Ryan, A. Carugo, L. Nezi, Y. Wei, H. Yang, M. D'Anca, L. Zhang, S. Gaddis,

- T. Gong, J.W. Horner, T.P. Heffernan, P. Jones, L.J. Cooper, H. Liang, H. Kantarjian, Y.A. Wang, L. Chin, C. Bueso-Ramos, G. Garcia-Manero, and R.A. DePinho, *Telomere dysfunction drives aberrant hematopoietic differentiation and myelodysplastic syndrome*. *Cancer Cell*, 2015. **27**(5): p. 644-57.
11. Chen, J., Y.R. Kao, D. Sun, T.I. Todorova, D. Reynolds, S.R. Narayanagari, C. Montagna, B. Will, A. Verma, and U. Steidl, *Myelodysplastic syndrome progression to acute myeloid leukemia at the stem cell level*, in *Nature Medicine*. 2019, Springer US. p. 103-110.
 12. Bowman, R.L., L. Busque, and R.L. Levine, *Clonal Hematopoiesis and Evolution to Hematopoietic Malignancies*, in *Cell Stem Cell*. 2018, Elsevier Inc. p. 157-170.
 13. Woll, P.S., U. Kjallquist, O. Chowdhury, H. Doolittle, D.C. Wedge, S. Thongjuea, R. Erlandsson, M. Ngara, K. Anderson, Q. Deng, A.J. Mead, L. Stenson, A. Giustacchini, S. Duarte, E. Giannoulatou, S. Taylor, M. Karimi, C. Scharenberg, T. Mortera-Blanco, I.C. Macaulay, S.A. Clark, I. Dybedal, D. Josefsen, P. Fenaux, P. Hokland, M.S. Holm, M. Cazzola, L. Malcovati, S. Tauro, D. Bowen, J. Boultwood, A. Pellagatti, J.E. Pimanda, A. Unnikrishnan, P. Vyas, G. Gohring, B. Schlegelberger, M. Tobiasson, G. Kvalheim, S.N. Constantinescu, C. Nerlov, L. Nilsson, P.J. Campbell, R. Sandberg, E. Papaemmanuil, E. Hellstrom-Lindberg, S. Linnarsson, and S.E. Jacobsen, *Myelodysplastic syndromes are propagated by rare and distinct human cancer stem cells in vivo*. *Cancer Cell*, 2014. **25**(6): p. 794-808.
 14. Gondek, L.P. and A.E. DeZern, *Assessing clonal haematopoiesis: clinical burdens and benefits of diagnosing myelodysplastic syndrome precursor states*, in *The Lancet Haematology*. 2020, Elsevier Ltd. p. e73-e81.
 15. Walter, M.J., D. Shen, L. Ding, J. Shao, D.C. Koboldt, K. Chen, D.E. Larson, M.D. McLellan, D. Dooling, R. Abbott, R. Fulton, V. Magrini, H. Schmidt, J. Kalicki-Veizer, M. O'Laughlin, X. Fan, M. Grillot, S. Witowski, S. Heath, J.L. Frater, W. Eades, M.

- Tomasson, P. Westervelt, J.F. DiPersio, D.C. Link, E.R. Mardis, T.J. Ley, R.K. Wilson, and T.A. Graubert, *Clonal architecture of secondary acute myeloid leukemia*. N Engl J Med, 2012. **366**(12): p. 1090-8.
16. da Silva-Coelho, P., L.I. Kroeze, K. Yoshida, T.N. Koorenhof-Scheele, R. Knops, L.T. van de Locht, A.O. de Graaf, M. Massop, S. Sandmann, M. Dugas, M.J. Stevens-Kroef, J. Cermak, Y. Shiraishi, K. Chiba, H. Tanaka, S. Miyano, T. de Witte, N.M.A. Blijlevens, P. Muus, G. Huls, B.A. van der Reijden, S. Ogawa, and J.H. Jansen, *Clonal evolution in myelodysplastic syndromes*. Nat Commun, 2017. **8**: p. 15099.
 17. Steensma, D.P., R. Bejar, S. Jaiswal, R.C. Lindsley, M.A. Sekeres, R.P. Hasserjian, and B.L. Ebert, *Clonal hematopoiesis of indeterminate potential and its distinction from myelodysplastic syndromes*, in *Blood*. 2015. p. 9-16.
 18. Haase, D., U. Germing, J. Schanz, M. Pfeilstocker, T. Nosslinger, B. Hildebrandt, A. Kundgen, M. Lubbert, R. Kunzmann, A.A. Giagounidis, C. Aul, L. Trumper, O. Krieger, R. Stauder, T.H. Muller, F. Wimazal, P. Valent, C. Fonatsch, and C. Steidl, *New insights into the prognostic impact of the karyotype in MDS and correlation with subtypes: evidence from a core dataset of 2124 patients*. Blood, 2007. **110**(13): p. 4385-95.
 19. Haferlach, T., Y. Nagata, V. Grossmann, Y. Okuno, U. Bacher, G. Nagae, S. Schnittger, M. Sanada, A. Kon, T. Alpermann, K. Yoshida, A. Roller, N. Nadarajah, Y. Shiraishi, Y. Shiozawa, K. Chiba, H. Tanaka, H.P. Koefler, H.U. Klein, M. Dugas, H. Aburatani, A. Kohlmann, S. Miyano, C. Haferlach, W. Kern, and S. Ogawa, *Landscape of genetic lesions in 944 patients with myelodysplastic syndromes*. Leukemia, 2014. **28**(2): p. 241-7.
 20. Papaemmanuil, E., M. Gerstung, L. Malcovati, S. Tauro, G. Gundem, P. Van Loo, C.J. Yoon, P. Ellis, D.C. Wedge, A. Pellagatti, A. Shlien, M.J. Groves, S.A. Forbes, K. Raine, J. Hinton, L.J. Mudie, S. McLaren, C. Hardy, C. Latimer, M.G. Della Porta, S. O'Meara, I. Ambaglio, A. Galli, A.P. Butler, G. Walldin, J.W. Teague, L. Quek, A. Sternberg, C.

- Gambacorti-Passerini, N.C. Cross, A.R. Green, J. Boultonwood, P. Vyas, E. Hellstrom-Lindberg, D. Bowen, M. Cazzola, M.R. Stratton, P.J. Campbell, and C. Chronic Myeloid Disorders Working Group of the International Cancer Genome, *Clinical and biological implications of driver mutations in myelodysplastic syndromes*. Blood, 2013. **122**(22): p. 3616-27; quiz 3699.
21. Ogawa, S., *Genetics of MDS*, in *Blood*. 2019. p. 1049-1059.
 22. Nagata, Y. and J.P. Maciejewski, *The functional mechanisms of mutations in myelodysplastic syndrome*. Leukemia, 2019. **33**(12): p. 2779-2794.
 23. Kantarjian, H., J.P. Issa, C.S. Rosenfeld, J.M. Bennett, M. Albitar, J. DiPersio, V. Klimek, J. Slack, C. de Castro, F. Ravandi, R. Helmer, 3rd, L. Shen, S.D. Nimer, R. Leavitt, A. Raza, and H. Saba, *Decitabine improves patient outcomes in myelodysplastic syndromes: results of a phase III randomized study*. Cancer, 2006. **106**(8): p. 1794-803.
 24. Silverman, L.R., D.R. McKenzie, B.L. Peterson, J.F. Holland, J.T. Backstrom, C.L. Beach, R.A. Larson, Cancer, and B. Leukemia Group, *Further analysis of trials with azacitidine in patients with myelodysplastic syndrome: studies 8421, 8921, and 9221 by the Cancer and Leukemia Group B*. J Clin Oncol, 2006. **24**(24): p. 3895-903.
 25. Issa, J.P., *DNA methylation as a therapeutic target in cancer*. Clin Cancer Res, 2007. **13**(6): p. 1634-7.
 26. Kordella, C., E. Lamprianidou, and I. Kotsianidis, *Mechanisms of Action of Hypomethylating Agents: Endogenous Retroelements at the Epicenter*. Front Oncol, 2021. **11**: p. 650473.
 27. Yoo, C.B. and P.A. Jones, *Epigenetic therapy of cancer: past, present and future*. Nat Rev Drug Discov, 2006. **5**(1): p. 37-50.

28. Stresemann, C., B. Brueckner, T. Musch, H. Stopper, and F. Lyko, *Functional diversity of DNA methyltransferase inhibitors in human cancer cell lines*. Cancer Res, 2006. **66**(5): p. 2794-800.
29. Zeidan, A.M., M. Stahl, M. DeVeaux, S. Giri, S. Huntington, N. Podoltsev, R. Wang, X. Ma, A.J. Davidoff, and S.D. Gore, *Counseling patients with higher-risk MDS regarding survival with azacitidine therapy: are we using realistic estimates?* Blood Cancer J, 2018. **8**(6): p. 55.
30. Garcia-Manero, G., K.S. Chien, and G. Montalban-Bravo, *Myelodysplastic syndromes: 2021 update on diagnosis, risk stratification and management*. Am J Hematol, 2020. **95**(11): p. 1399-1420.
31. Greenberg, P.L., H. Tuechler, J. Schanz, G. Sanz, G. Garcia-Manero, F. Sole, J.M. Bennett, D. Bowen, P. Fenau, F. Dreyfus, H. Kantarjian, A. Kuendgen, A. Levis, L. Malcovati, M. Cazzola, J. Cermak, C. Fonatsch, M.M. Le Beau, M.L. Slovak, O. Krieger, M. Luebbert, J. Maciejewski, S.M. Magalhaes, Y. Miyazaki, M. Pfeilstocker, M. Sekeres, W.R. Sperr, R. Stauder, S. Tauro, P. Valent, T. Vallespi, A.A. van de Loosdrecht, U. Germing, and D. Haase, *Revised international prognostic scoring system for myelodysplastic syndromes*. Blood, 2012. **120**(12): p. 2454-65.
32. Greenberg, P., C. Cox, M.M. LeBeau, P. Fenau, P. Morel, G. Sanz, M. Sanz, T. Vallespi, T. Hamblin, D. Oscier, K. Ohyashiki, K. Toyama, C. Aul, G. Mufti, and J. Bennett, *International scoring system for evaluating prognosis in myelodysplastic syndromes*. Blood, 1997. **89**(6): p. 2079-88.
33. Takahashi, K., K. Patel, C. Bueso-Ramos, J. Zhang, C. Gumbs, E. Jabbour, T. Kadia, M. Andreff, M. Konopleva, C. DiNardo, N. Daver, J. Cortes, Z. Estrov, A. Futreal, H. Kantarjian, and G. Garcia-Manero, *Clinical implications of TP53 mutations in myelodysplastic syndromes treated with hypomethylating agents*. Oncotarget, 2016. **7**(12): p. 14172-87.

34. Corces-Zimmerman, M.R., W.J. Hong, I.L. Weissman, B.C. Medeiros, and R. Majeti, *Preleukemic mutations in human acute myeloid leukemia affect epigenetic regulators and persist in remission*. Proc Natl Acad Sci U S A, 2014. **111**(7): p. 2548-53.
35. Makishima, H., T. Yoshizato, K. Yoshida, M.A. Sekeres, T. Radivoyevitch, H. Suzuki, B. Przychodzen, Y. Nagata, M. Meggendorfer, M. Sanada, Y. Okuno, C. Hirsch, T. Kuzmanovic, Y. Sato, A. Sato-Otsubo, T. LaFramboise, N. Hosono, Y. Shiraishi, K. Chiba, C. Haferlach, W. Kern, H. Tanaka, Y. Shiozawa, I. Gomez-Segui, H.D. Hussein, S. Thota, K.M. Guinta, B. Dienes, T. Nakamaki, S. Miyawaki, Y. Sauntharajah, S. Chiba, S. Miyano, L.Y. Shih, T. Haferlach, S. Ogawa, and J.P. Maciejewski, *Dynamics of clonal evolution in myelodysplastic syndromes*. Nat Genet, 2017. **49**(2): p. 204-212.
36. Tahir, S.K., M.L. Smith, P. Hessler, L.R. Rapp, K.B. Idler, C.H. Park, J.D. Levenson, and L.T. Lam, *Potential mechanisms of resistance to venetoclax and strategies to circumvent it*. BMC Cancer, 2017. **17**(1): p. 399.
37. Chen, C., L.C. Edelstein, and C. Gelinas, *The Rel/NF-kappaB family directly activates expression of the apoptosis inhibitor Bcl-x(L)*. Mol Cell Biol, 2000. **20**(8): p. 2687-95.
38. Teh, T.C., N.Y. Nguyen, D.M. Moujalled, D. Segal, G. Pomilio, S. Rijal, A. Jabbour, K. Cummins, K. Lackovic, P. Blombery, E. Thompson, P.G. Ekert, G. Lessene, S.P. Glaser, D.C.S. Huang, A.W. Roberts, M.A. Guthridge, and A.H. Wei, *Enhancing venetoclax activity in acute myeloid leukemia by co-targeting MCL1*. Leukemia, 2018. **32**(2): p. 303-312.
39. Moujalled, D.M., G. Pomilio, C. Ghiurau, A. Ivey, J. Salmon, S. Rijal, S. Macrauld, L. Zhang, T.C. Teh, I.S. Tiong, P. Lan, M. Chanrion, A. Claperon, F. Rocchetti, A. Zichi, L. Kraus-Berthier, Y. Wang, E. Halilovic, E. Morris, F. Colland, D. Segal, D. Huang, A.W. Roberts, A.L. Maragno, G. Lessene, O. Geneste, and A.H. Wei, *Combining BH3-*

- mimetics to target both BCL-2 and MCL1 has potent activity in pre-clinical models of acute myeloid leukemia*. *Leukemia*, 2019. **33**(4): p. 905-917.
40. Ramsey, H.E., M.A. Fischer, T. Lee, A.E. Gorska, M.P. Arrate, L. Fuller, K.L. Boyd, S.A. Strickland, J. Sensintaffar, L.J. Hogdal, G.D. Ayers, E.T. Olejniczak, S.W. Fesik, and M.R. Savona, *A Novel MCL1 Inhibitor Combined with Venetoclax Rescues Venetoclax-Resistant Acute Myelogenous Leukemia*. *Cancer Discov*, 2018. **8**(12): p. 1566-1581.
 41. Rathmell, J.C. and C.B. Thompson, *Pathways of apoptosis in lymphocyte development, homeostasis, and disease*. *Cell*, 2002. **109 Suppl**: p. S97-107.
 42. Letai, A., M.C. Bassik, L.D. Walensky, M.D. Sorcinelli, S. Weiler, and S.J. Korsmeyer, *Distinct BH3 domains either sensitize or activate mitochondrial apoptosis, serving as prototype cancer therapeutics*. *Cancer Cell*, 2002. **2**(3): p. 183-92.
 43. Singh, R., A. Letai, and K. Sarosiek, *Regulation of apoptosis in health and disease: the balancing act of BCL-2 family proteins*, in *Nature Reviews Molecular Cell Biology*. 2019, Springer US. p. 175-193.
 44. Carneiro, B.A. and W.S. El-Deiry, *Targeting apoptosis in cancer therapy*, in *Nature Reviews Clinical Oncology*. 2020, Springer US.
 45. Hanahan, D. and R.A. Weinberg, *Hallmarks of cancer: the next generation*. *Cell*, 2011. **144**(5): p. 646-74.
 46. Ashkenazi, A., W.J. Fairbrother, J.D. Levenson, and A.J. Souers, *From basic apoptosis discoveries to advanced selective BCL-2 family inhibitors*. *Nat Rev Drug Discov*, 2017. **16**(4): p. 273-284.
 47. Souers, A.J., J.D. Levenson, E.R. Boghaert, S.L. Ackler, N.D. Catron, J. Chen, B.D. Dayton, H. Ding, S.H. Enschede, W.J. Fairbrother, D.C.S. Huang, S.G. Hymowitz, S. Jin, S.L. Khaw, P.J. Kovar, L.T. Lam, J. Lee, H.L. Maecker, K.C. Marsh, K.D. Mason, M.J. Mitten, P.M. Nimmer, A. Oleksijew, C.H. Park, C.M. Park, D.C. Phillips, A.W. Roberts, D. Sampath, J.F. Seymour, M.L. Smith, G.M. Sullivan, S.K. Tahir, C. Tse, M.D.

- Wendt, Y. Xiao, J.C. Xue, H. Zhang, R.A. Humerickhouse, S.H. Rosenberg, and S.W. Elmore, *ABT-199, a potent and selective BCL-2 inhibitor, achieves antitumor activity while sparing platelets*, in *Nature Medicine*. 2013, Nature Publishing Group. p. 202-208.
48. Deeks, E.D., *Venetoclax: First Global Approval*. *Drugs*, 2016. **76**(9): p. 979-87.
 49. DiNardo, C.D., K. Pratz, V. Pullarkat, B.A. Jonas, M. Arellano, P.S. Becker, O. Frankfurt, M. Konopleva, A.H. Wei, H.M. Kantarjian, T. Xu, W.J. Hong, B. Chyla, J. Potluri, D.A. Pollyea, and A. Letai, *Venetoclax combined with decitabine or azacitidine in treatment-naïve, elderly patients with acute myeloid leukemia*. *Blood*, 2019. **133**(1): p. 7-17.
 50. Carter, B.Z., P.Y. Mak, W. Tao, M. Warmoes, P.L. Lorenzi, D. Mak, V. Ruvoilo, L. Tan, J. Cidado, L. Drew, and M. Andreeff, *Targeting MCL-1 dysregulates cell metabolism and leukemia-stroma interactions and resensitizes acute myeloid leukemia to BCL-2 inhibition*. *Haematologica*, 2020. **Online ahead of print**.
 51. Konopleva, M., D.A. Pollyea, J. Potluri, B. Chyla, L. Hogdal, T. Busman, E. McKeegan, A.H. Salem, M. Zhu, J.L. Ricker, W. Blum, C.D. DiNardo, T. Kadia, M. Dunbar, R. Kirby, N. Falotico, J. Levenson, R. Humerickhouse, M. Mabry, R. Stone, H. Kantarjian, and A. Letai, *Efficacy and Biological Correlates of Response in a Phase II Study of Venetoclax Monotherapy in Patients with Acute Myelogenous Leukemia*. *Cancer Discov*, 2016. **6**(10): p. 1106-1117.
 52. Bose, P., V. Gandhi, and M. Konopleva, *Pathways and mechanisms of venetoclax resistance*, in *Leukemia and Lymphoma*. 2017. p. 2026-2039.
 53. Caenepeel, S., S.P. Brown, B. Belmontes, G. Moody, K.S. Keegan, D. Chui, D.A. Whittington, X. Huang, L. Poppe, A.C. Cheng, M. Cardozo, J. Houze, Y. Li, B. Lucas, N.A. Paras, X. Wang, J.P. Taygerly, M. Vimolratana, M. Zancanella, L. Zhu, E. Cajulis, T. Osgood, J. Sun, L. Damon, R.K. Egan, P. Greninger, J.D. McClanaghan, J. Gong, D. Moujalled, G. Pomilio, P. Beltran, C.H. Benes, A.W. Roberts, D.C. Huang, A. Wei, J.

- Canon, A. Coxon, and P.E. Hughes, *AMG 176, a selective MCL1 inhibitor, is effective in hematologic cancer models alone and in combination with established therapies*, in *Cancer Discovery*. 2018. p. 1582-1597.
54. Nangia, V., F.M. Siddiqui, S. Caenepeel, D. Timonina, S.J. Bilton, N. Phan, M. Gomez-Caraballo, H.L. Archibald, C. Li, C. Fraser, D. Rigas, K. Vajda, L.A. Ferris, M. Lanuti, C.D. Wright, K.A. Raskin, D.P. Cahill, J.H. Shin, C. Keyes, L.V. Sequist, Z. Piotrowska, A.F. Farago, C.G. Azzoli, J.F. Gainor, K.A. Sarosiek, S.P. Brown, A. Coxon, C.H. Benes, P.E. Hughes, and A.N. Hata, *Exploiting MCL1 Dependency with Combination MEK + MCL1 Inhibitors Leads to Induction of Apoptosis and Tumor Regression in KRAS-Mutant Non-Small Cell Lung Cancer*. *Cancer Discov*, 2018. **8**(12): p. 1598-1613.
 55. Kohlhapp, F.J., D. Haribhai, R. Mathew, R. Duggan, P.A. Ellis, R. Wang, E.A. Lasater, Y. Shi, N. Dave, J.J. Riehm, V.A. Robinson, A.D. Do, Y. Li, C.J. Orr, D. Sampath, A. Raval, M. Merchant, A. Bhathena, A.H. Salem, K.M. Hamel, J.D. Levenson, C. Donawho, W.N. Pappano, and T. Uziel, *Venetoclax Increases Intratumoral Effector T Cells and Antitumor Efficacy in Combination with Immune Checkpoint Blockade*. *Cancer Discov*, 2021. **11**(1): p. 68-79.
 56. Lee, J., D.H. Khan, R. Hurren, M. Xu, Y. Na, H. Kang, S. Mirali, X. Wang, M.V. Gronda, Y. Jitkova, N. MacLean, A. Arruda, Z. Alaniz, M.Y. Konopleva, M. Andreeff, M.D. Minden, L. Zhang, and A.D. Schimmer, *Venetoclax enhances T cell-mediated anti-leukemic activity by increasing ROS production*. *Blood*, 2021.
 57. Waldman, A.D., J.M. Fritz, and M.J. Lenardo, *A guide to cancer immunotherapy: from T cell basic science to clinical practice*, in *Nature Reviews Immunology*. 2020, Nature Research. p. 651-668.
 58. Germain, R.N., *T-cell development and the CD4-CD8 lineage decision*. *Nat Rev Immunol*, 2002. **2**(5): p. 309-22.

59. Gattinoni, L., D.E. Speiser, M. Lichterfeld, and C. Bonini, *T memory stem cells in health and disease*. Nat Med, 2017. **23**(1): p. 18-27.
60. Kumar, B.V., T.J. Connors, and D.L. Farber, *Human T Cell Development, Localization, and Function throughout Life*. Immunity, 2018. **48**(2): p. 202-213.
61. Okhrimenko, A., J.R. Grun, K. Westendorf, Z. Fang, S. Reinke, P. von Roth, G. Wassilew, A.A. Kuhl, R. Kudernatsch, S. Demski, C. Scheibenbogen, K. Tokoyoda, M.A. McGrath, M.J. Raftery, G. Schonrich, A. Serra, H.D. Chang, A. Radbruch, and J. Dong, *Human memory T cells from the bone marrow are resting and maintain long-lasting systemic memory*. Proc Natl Acad Sci U S A, 2014. **111**(25): p. 9229-34.
62. Farber, D.L., N.A. Yudanin, and N.P. Restifo, *Human memory T cells: generation, compartmentalization and homeostasis*. Nat Rev Immunol, 2014. **14**(1): p. 24-35.
63. Bettelli, E., Y. Carrier, W. Gao, T. Korn, T.B. Strom, M. Oukka, H.L. Weiner, and V.K. Kuchroo, *Reciprocal developmental pathways for the generation of pathogenic effector TH17 and regulatory T cells*. Nature, 2006. **441**(7090): p. 235-8.
64. Liu, H., J. Yang, Y. Yuan, Z. Xia, M. Chen, L. Xie, X. Ma, J. Wang, S. Ouyang, Q. Wu, F. Yu, X. Zhou, Y. Yang, Y. Cao, J. Hu, and B. Yin, *Regulation of Mcl-1 by constitutive activation of NF-kappaB contributes to cell viability in human esophageal squamous cell carcinoma cells*. BMC Cancer, 2014. **14**: p. 98.
65. Chen, Y., R. Jacamo, Y.X. Shi, R.Y. Wang, V.L. Battula, S. Konoplev, D. Strunk, N.A. Hofmann, A. Reinisch, M. Konopleva, and M. Andreeff, *Human extramedullary bone marrow in mice: a novel in vivo model of genetically controlled hematopoietic microenvironment*. Blood, 2012. **119**(21): p. 4971-80.
66. Will, B., L. Zhou, T.O. Vogler, S. Ben-Neriah, C. Schinke, R. Tamari, Y. Yu, T.D. Bhagat, S. Bhattacharyya, L. Barreyro, C. Heuck, Y. Mo, S. Parekh, C. McMahon, A. Pellagatti, J. Boulwood, C. Montagna, L. Silverman, J. Maciejewski, J.M. Greally, B.H. Ye, A.F. List, C. Steidl, U. Steidl, and A. Verma, *Stem and progenitor cells in*

- myelodysplastic syndromes show aberrant stage-specific expansion and harbor genetic and epigenetic alterations.* Blood, 2012. **120**(10): p. 2076-86.
67. Doulatov, S., F. Notta, K. Eppert, L.T. Nguyen, P.S. Ohashi, and J.E. Dick, *Revised map of the human progenitor hierarchy shows the origin of macrophages and dendritic cells in early lymphoid development.* Nat Immunol, 2010. **11**(7): p. 585-93.
 68. Notta, F., S. Zandi, N. Takayama, S. Dobson, O.I. Gan, G. Wilson, K.B. Kaufmann, J. McLeod, E. Laurenti, C.F. Dunant, J.D. McPherson, L.D. Stein, Y. Dror, and J.E. Dick, *Distinct routes of lineage development reshape the human blood hierarchy across ontogeny.* Science, 2016. **351**(6269): p. aab2116.
 69. Gorgens, A., S. Radtke, M. Mollmann, M. Cross, J. Durig, P.A. Horn, and B. Giebel, *Revision of the human hematopoietic tree: granulocyte subtypes derive from distinct hematopoietic lineages.* Cell Rep, 2013. **3**(5): p. 1539-52.
 70. Stuart, T., A. Butler, P. Hoffman, C. Hafemeister, E. Papalexi, W.M. Mauck, 3rd, Y. Hao, M. Stoeckius, P. Smibert, and R. Satija, *Comprehensive Integration of Single-Cell Data.* Cell, 2019. **177**(7): p. 1888-1902 e21.
 71. Bodenmiller, B., E.R. Zunder, R. Finck, T.J. Chen, E.S. Savig, R.V. Bruggner, E.F. Simonds, S.C. Bendall, K. Sachs, P.O. Krutzik, and G.P. Nolan, *Multiplexed mass cytometry profiling of cellular states perturbed by small-molecule regulators.* Nat Biotechnol, 2012. **30**(9): p. 858-67.
 72. DiNardo, C.D., C.R. Rausch, C. Benton, T. Kadia, N. Jain, N. Pemmaraju, N. Daver, W. Covert, K.R. Marx, M. Mace, E. Jabbour, J. Cortes, G. Garcia-Manero, F. Ravandi, K.N. Bhalla, H. Kantarjian, and M. Konopleva, *Clinical experience with the BCL2-inhibitor venetoclax in combination therapy for relapsed and refractory acute myeloid leukemia and related myeloid malignancies.* Am J Hematol, 2018. **93**(3): p. 401-407.
 73. Matsuoka, A., A. Tochigi, M. Kishimoto, T. Nakahara, T. Kondo, T. Tsujioka, T. Tasaka, Y. Tohyama, and K. Tohyama, *Lenalidomide induces cell death in an MDS-derived cell*

- line with deletion of chromosome 5q by inhibition of cytokinesis. Leukemia, 2010. 24(4): p. 748-55.*
74. Chen, J., Y.R. Kao, D. Sun, T.I. Todorova, D. Reynolds, S.R. Narayanagari, C. Montagna, B. Will, A. Verma, and U. Steidl, *Myelodysplastic syndrome progression to acute myeloid leukemia at the stem cell level. Nat Med, 2019. 25(1): p. 103-110.*
 75. Nechiporuk, T., S.E. Kurtz, O. Nikolova, T. Liu, C.L. Jones, A. D'Alessandro, R. Culp-Hill, A. d'Almeida, S.K. Joshi, M. Rosenberg, C.E. Tognon, A.V. Danilov, B.J. Druker, B.H. Chang, S.K. McWeeney, and J.W. Tyner, *The TP53 Apoptotic Network Is a Primary Mediator of Resistance to BCL2 Inhibition in AML Cells. Cancer Discov, 2019. 9(7): p. 910-925.*
 76. Sallman, D.A., A.E. DeZern, G. Garcia-Manero, D.P. Steensma, G.J. Roboz, M.A. Sekeres, T. Cluzeau, K.L. Sweet, A. McLemore, K.L. McGraw, J. Puskas, L. Zhang, J. Yao, Q. Mo, L. Nardelli, N.H. Al Ali, E. Padron, G. Korbel, E.C. Attar, H.M. Kantarjian, J.E. Lancet, P. Fenaux, A.F. List, and R.S. Komrokji, *Eprenetapopt (APR-246) and Azacitidine in TP53-Mutant Myelodysplastic Syndromes. J Clin Oncol, 2021. 39(14): p. 1584-1594.*
 77. Chapman, N.M., M.R. Boothby, and H. Chi, *Metabolic coordination of T cell quiescence and activation. Nat Rev Immunol, 2020. 20(1): p. 55-70.*
 78. Lee, H.G., M.Z. Cho, and J.M. Choi, *Bystander CD4(+) T cells: crossroads between innate and adaptive immunity. Exp Mol Med, 2020. 52(8): p. 1255-1263.*
 79. Jansen, C.S., N. Prokhnevskaya, V.A. Master, M.G. Sanda, J.W. Carlisle, M.A. Bilen, M. Cardenas, S. Wilkinson, R. Lake, A.G. Sowalsky, R.M. Valanparambil, W.H. Hudson, D. McGuire, K. Melnick, A.I. Khan, K. Kim, Y.M. Chang, A. Kim, C.P. Filson, M. Alemozaffar, A.O. Osunkoya, P. Mullane, C. Ellis, R. Akondy, S.J. Im, A.O. Kamphorst, A. Reyes, Y. Liu, and H. Kissick, *An intra-tumoral niche maintains and differentiates stem-like CD8 T cells. Nature, 2019. 576(7787): p. 465-470.*

80. Gattinoni, L., E. Lugli, Y. Ji, Z. Pos, C.M. Paulos, M.F. Quigley, J.R. Almeida, E. Gostick, Z. Yu, C. Carpenito, E. Wang, D.C. Douek, D.A. Price, C.H. June, F.M. Marincola, M. Roederer, and N.P. Restifo, *A human memory T cell subset with stem cell-like properties*. Nat Med, 2011. **17**(10): p. 1290-7.
81. Liu, Q., Z. Sun, and L. Chen, *Memory T cells: strategies for optimizing tumor immunotherapy*. Protein Cell, 2020. **11**(8): p. 549-564.
82. De Simone, M., G. Rossetti, and M. Pagani, *Single Cell T Cell Receptor Sequencing: Techniques and Future Challenges*. Front Immunol, 2018. **9**: p. 1638.
83. Yi, J.S., M.A. Cox, and A.J. Zajac, *T-cell exhaustion: characteristics, causes and conversion*. Immunology, 2010. **129**(4): p. 474-81.
84. Wherry, E.J. and M. Kurachi, *Molecular and cellular insights into T cell exhaustion*. Nat Rev Immunol, 2015. **15**(8): p. 486-99.
85. Chen, J.J., M. Kwak, and R. Fan, *Single-Cell Cytokine Profiling to Investigate Cellular Functional Diversity in Hematopoietic Malignancies*. Methods Mol Biol, 2016. **1465**: p. 243-54.

VITA

Shuaitong Chen was born in China on October 25th, 1997. After graduating from True Light High School in Guangzhou, China in 2015, Shuaitong attended Wesleyan College in Macon, Georgia to pursue a Bachelor's degree in Biology. There, Shuaitong joined Dr. Barry Rhoades research study to conduct her Honors Thesis project. She graduated from Wesleyan College in May 2019 and received the degree of Bachelor of Art with a major in Biology, *magna cum laude*. Later in August, she entered the University of Texas MD Anderson Cancer Center UTHealth Graduate School of Biomedical Sciences to pursue a Master's degree in Biomedical Sciences. She joined the laboratory of Dr. Simona Colla in October, 2019 in the Department of Leukemia at the University of Texas MD Anderson Cancer Center, Houston, Texas and is affiliated with the Cancer Biology Graduate Program.